Get Full Access and More at ExpertConsult.com

EDITION 9

SABISTON & SPENCER

SURGERY *of the* CHEST

Frank W. Sellke
Pedro J. del Nido
Scott J. Swanson

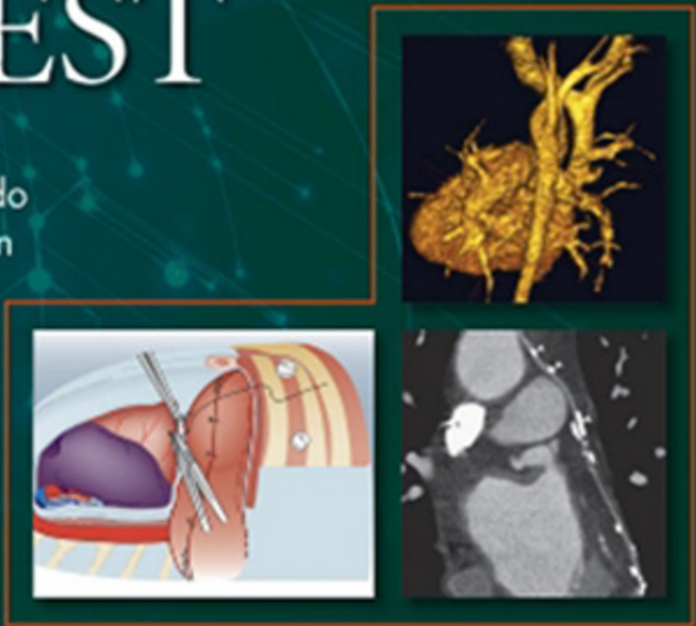

ELSEVIER

VOLUME ONE

ExpertConsult.com

EDITION 9

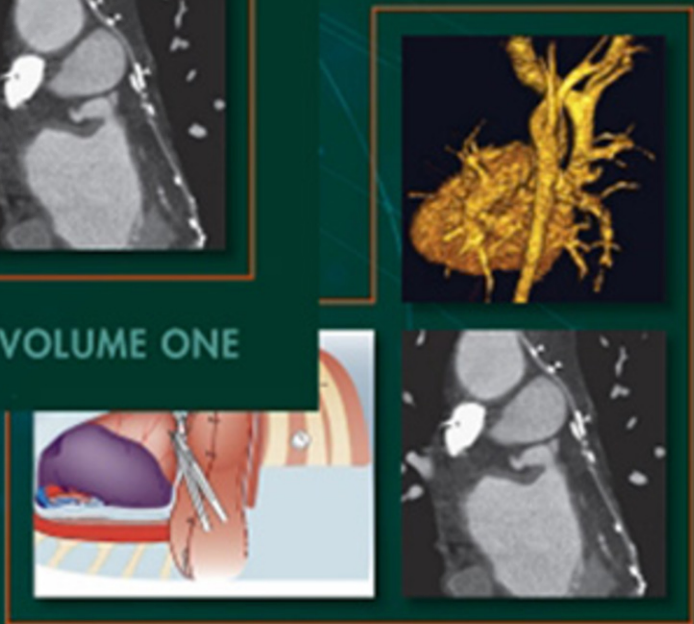

ELSEVIER

VOLUME TWO

2-Volume Set

SABISTON & SPENCER

SURGERY *of the* CHEST

This page intentionally left blank

EDITION 9

SABISTON & SPENCER

SURGERY *of the* CHEST

Frank W. Sellke, MD

Karl Karlson & Gloria Karlson Professor and Chief of Cardiothoracic Surgery
Warren Alpert Medical School of Brown University and Rhode Island Hospital
Director, Lifespan Cardiovascular Institute
Providence, Rhode Island

Pedro J. del Nido, MD

William E. Ladd Professor of Surgery
Harvard Medical School
Chairman, Department of Cardiac Surgery
Boston Children's Hospital
Boston, Massachusetts

Scott J. Swanson, MD

Director, Minimally Invasive Thoracic Surgery
Brigham and Women's Hospital
Vice Chair, Cancer Affairs
Department of Surgery, Brigham and Women's Hospital
Chief Surgical Officer
Dana-Farber Cancer Institute
Professor of Surgery
Harvard Medical School
Boston, Massachusetts

ELSEVIER

ELSEVIER

1600 John F. Kennedy Blvd.
Ste 1800
Philadelphia, PA 19103-2899

SABISTON & SPENCER SURGERY OF THE CHEST, NINTH EDITION ISBN: 978-0-323-24126-7

Notices

Knowledge and best practice in this field are constantly changing. As new research and experience broaden our understanding, changes in research methods, professional practices, or medical treatment may become necessary.

Practitioners and researchers must always rely on their own experience and knowledge in evaluating and using any information, methods, compounds, or experiments described herein. In using such information or methods they should be mindful of their own safety and the safety of others, including parties for whom they have a professional responsibility.

With respect to any drug or pharmaceutical products identified, readers are advised to check the most current information provided (i) on procedures featured or (ii) by the manufacturer of each product to be administered, to verify the recommended dose or formula, the method and duration of administration, and contraindications. It is the responsibility of practitioners, relying on their own experience and knowledge of their patients, to make diagnoses, to determine dosages and the best treatment for each individual patient, and to take all appropriate safety precautions.

To the fullest extent of the law, neither the Publisher nor the authors, contributors, or editors assume any liability for any injury and/or damage to persons or property as a matter of products liability, negligence or otherwise, or from any use or operation of any methods, products, instructions, or ideas contained in the material herein.

Library of Congress Cataloging-in-Publication Data

Sabiston & Spencer surgery of the chest / [edited by] Frank W. Sellke, Pedro J. del Nido, Scott J. Swanson.—Ninth edition.
p. ; cm.
Sabiston and Spencer surgery of the chest
Surgery of the chest
Includes bibliographical references and index.
ISBN 978-0-323-24126-7 (hardcover : alk. paper)
I. Sellke, Frank W., editor. II. Del Nido, Pedro J., editor. III. Swanson, Scott J., editor. IV. Title: Sabiston and Spencer surgery of the chest. V. Title: Surgery of the chest.
[DNLM: 1. Thoracic Surgical Procedures—methods. WF 980]
RD536
617.5′4—dc23

2015020235

Publishing Manager: Michael Houston
Senior Content Development Manager: Maureen Iannuzzi
Senior Content Development Specialist: Joan Ryan
Publishing Services Manager: Catherine Jackson
Project Manager: Rhoda Howell
Design Direction: Maggie Reid

Printed in China

Last digit is the print number: 9 8 7 6 5 4 3 2 1

To my wife, Amy, who gives me love, inspiration,
and unwavering support and to our children,
Michelle, Eric, Nicholas, and Amanda.
They provide us with unlimited pleasure.

FWS

To Martha, my loving wife, and to my children,
Alexander and his wife Erika, to Sara, Daniel,
Elizabeth, and to my grandson Matthew who keeps
reminding us of the important things in life.
Thank you.

PJD

To my mother, Anne Parkhurst, and my wife,
Donna, and our children, Whit, Kate, and Maggie:
I am very appreciative and grateful for the guidance,
love, and support; gives meaning to all of what I do.
To my patients: the inspiration to work hard and do
better every day.

SJS

Contributors

Brian G. Abbott, MD
Associate Professor of Medicine
Cardiovascular Institute
Warren Alpert Medical School of Brown University
Providence, Rhode Island

J. Dawn Abbott, MD
Associate Professor of Medicine
Director, Interventional Cardiology
Fellowship Training Program
Warren Alpert Medical School of Brown University
Interventional Cardiologist
Rhode Island Hospital
Providence, Rhode Island

David H. Adams, MD
Professor and Chairman
Department of Cardiovascular Surgery
The Mount Sinai Medical Center
New York, New York

Talal Al-Atassi, MD, CM, MPH
Chief Resident
Division of Cardiac Surgery
University of Ottawa Heart Institute
Ottawa, Ontario, Canada

Ali Al-Dameh, MD
Clinical Fellow in Thoracic Surgery
Brigham and Women's Hospital
Boston, Massachusetts

Mark S. Allen, MD
Professor of Surgery
Thoracic Surgery
Mayo Clinic
Rochester, Minnesota

Nasser K. Altorki, MB, BCh
Professor of Cardiothoracic Surgery
Weill Cornell Medical College
Chief, Division of Thoracic Surgery
Cardiothoracic Surgery
New York Presbyterian Hospital/Weill Cornell Medical College
New York, New York

Jatin Anand, MD
Michael E. DeBakey Department of Surgery
Baylor College of Medicine
Cardiovascular Research
Center for Cardiac Support
Texas Heart Institute
Houston, Texas

Robert H. Anderson, BSc, MD, FRC Path
Emeritus Professor
Institute of Child Health
University College
London, United Kingdom;
Visiting Professor
Division of Pediatric Cardiology
Medical University of South Carolina
Charleston, South Carolina;
Visiting Professor
Institute of Human Genetics
Newcastle University
Newcastle Upon Tyne, United Kingdom

Masaki Anraku, MD, MSc
Assistant Professor
Department of Thoracic Surgery
Graduate School of Medicine
The University of Tokyo
Tokyo, Japan

Anelechi C. Anyanwu, MD
Professor and Vice Chairman
Department of Cardiovascular Surgery
The Mount Sinai Medical Center
New York, New York

Amit Arora, MD
Department of Cardiovascular Surgery
The Mount Sinai Medical Center
New York, New York

Erle H. Austin, III, MD
Professor and Vice Chairman
Department of Cardiovascular and Thoracic Surgery
University of Louisville
Chief, Cardiothoracic Surgery
Kosair Children's Hospital
Louisville, Kentucky

Eric H. Awtry, MD
Associate Professor of Medicine
Boston University School of Medicine
Vice Chair for Clinical Affairs
Division of Cardiology
Boston Medical Center
Boston, Massachusetts

Emile A. Bacha, MD, FACS
Chief, Division of Cardiothoracic and Vascular Surgery
Department of Surgery
Columbia University Medical Center
New York Presbyterian Hospital
New York, New York

Leah M. Backhus, MD
Assistant Professor
Division of Cardiothoracic Surgery
University of Washington
Seattle, Washington

Jayant Bagai, MD
Assistant Professor of Medicine
Division of Cardiovascular Medicine
Vanderbilt University Medical Center
Nashville, Tennessee

Richard Baillot, MD, FRCSC
Institut Universitaire de Cardiologie et de Pneumologie de Québec
Québec City, Québec, Canada

Christopher W. Baird, MD
Assistant Professor of Surgery
Harvard Medical School
Associate in Cardiac Surgery
Boston Children's Hospital
Boston, Massachusetts

David J. Barron, MD, FRCP, FRCS(CT)
Consultant Cardiac Surgeon
Birmingham Children's Hospital
NHS Foundation Trust
Birmingham, United Kingdom

Joseph E. Bavaria, MD
Brooke Roberts/William Maul Measey Professor of Surgery
Vice Chair, Division of Cardiovascular Surgery
Director, Thoracic Aortic Surgery
Department of Surgery
Division of Cardiovascular Surgery
University of Pennsylvania
Hospital of University of Pennsylvania
Philadelphia, Pennsylvania

Jose M. Bernal, MD, PhD
Consultant and Professor of Surgery
Department of Cardiovascular Surgery
Hospital Valdecilla
University of Cantabria
Santander, Spain

Valentino J. Bianco, DO, MPH
Research Fellow, Thoracic Surgery
Department of Cardiothoracic Surgery
University of Pittsburgh School of Medicine
University of Pittsburgh Medical Center
Pittsburgh, Pennsylvania

David P. Bichell, MD
Cornelius Vanderbilt Chair in Surgery
Professor of Surgery
Cardiac Surgery
Vanderbilt University School of Medicine
Nashville, Tennessee

Sigurbjorn Birgisson, MD
Department of Gastroenterology
Digestive Disease Institute
Cleveland Clinic
Cleveland, Ohio

Nick J.R. Blackburn, BSc
Division of Cardiac Surgery
University of Ottawa Heart Institute
Department of Cellular and Molecular Medicine
University of Ottawa
Ottawa, Ontario, Canada

Johannes Bonatti, MD
Chairman, Department of Cardiothoracic Surgery
Cleveland Clinic Abu Dhabi
Abu Dhabi, United Arab Emirates

Munir Boodhwani, MD, MMSc
Associate Professor
Division of Cardiac Surgery
University of Ottawa Heart Institute
Ottawa, Ontario, Canada

Edward L. Bove, MD
Helen F. and Marvin M. Kirsh Professor of Cardiac Surgery
Chair, Department of Cardiac Surgery
Professor of Cardiac Surgery
Professor of Pediatrics and Communicable Disease
University of Michigan
Ann Arbor, Michigan

William J. Brawn, CBE, FRCS, FRACS
Consultant Cardiac Surgeon
Birmingham Children's Hospital
NHS Foundation Trust
Birmingham, United Kingdom

Christian P. Brizard, MD
Associate Professor
University of Melbourne Faculty of Medicine, Dentistry
Health Sciences School of Medicine
Cardiac Surgery Unit
Royal Children's Hospital
Melbourne, Victoria, Australia

Julie A. Brothers, MD
Assistant Professor of Pediatrics
Perelman School of Medicine
University of Pennsylvania
Attending Physician, Cardiology
Medical Director, Coronary Anomaly Management Program
Medical Director, Lipid Heart Clinic
The Children's Hospital of Philadelphia
Philadelphia, Pennsylvania

Lisa M. Brown, MD, MAS
Cardiothoracic Surgery Fellow
Division of Cardiothoracic Surgery
Washington University
St. Louis, Missouri

Ayesha S. Bryant, MD
Assistant Professor of Surgery
Division of Cardiothoracic Surgery
University of Alabama at Birmingham
Birmingham, Alabama

Harold M. Burkhart, MD
Professor of Surgery
Section of Cardiothoracic Surgery
The University of Oklahoma Health Sciences School of Medicine
Director of Pediatric Cardiovascular Surgery
Medical Director of Pediatric Cardiovascular Surgical Services
The Children's Hospital
Oklahoma City, Oklahoma

Christopher A. Caldarone, MD, FRCSC
Cardiovascular Surgery
The Hospital for Sick Children
Toronto, Ontario, Canada

Jeremy W. Cannon, MD, SM, FACS
Lieutenant Colonel, U.S. Air Force
Chief, Trauma and Critical Care
San Antonio Military Medical Center
San Antonio, Texas
Associate Professor of Surgery
Uniformed Services University of the Health Sciences
Bethesda, Maryland

Justine M. Carr, MD
Chief Medical Officer
Steward Health Care System
Senior Director, Department of Clinical Resource Management
Beth Israel Deaconess Medical Center
Boston, Massachusetts

Serenella Castelvecchio, MD
Department of Cardiac Surgery
IRCCS Policlinico San Donato
Milan, Italy

Javier G. Castillo, MD
Department of Cardiovascular Surgery
The Mount Sinai Medical Center
New York, New York

Frank Cecchin, MD
Professor of Pediatrics
Pediatric Cardiology
New York University
New York, New York

Robert J. Cerfolio, MD
Chief of Thoracic Surgery
Professor of Cardiothoracic Surgery
University of Alabama at Birmingham
Birmingham, Alabama

A. Alfred Chahine, MD
Associate Professor of Surgery and Pediatrics
George Washington University School of Medicine
Attending Surgeon
Children's National Medical Center
Chief of Pediatric Surgery
MedStar Georgetown University Hospital
Washington, DC

Elliot L. Chaikof, MD, PhD
Johnson and Johnson Professor of Surgery
Chairman, Roberta and Stephen R. Weiner Department of Surgery
Harvard Medical School
Surgeon-in-Chief
Beth Israel Deaconess Medical Center
Boston, Massachusetts

Vincent Chan, MD, MPH
Assistant Professor
Division of Cardiac Surgery
University of Ottawa Heart Institute
Ottawa, Ontario, Canada

Sunit-Preet Chaudhry, MD
Cardiovascular Institute
Warren Alpert Medical School of Brown University
Providence, Rhode Island

Frederick Y. Chen, MD, PhD
Associate Professor of Cardiac Surgery
Harvard Medical School
Department of Surgery
Division of Cardiac Surgery
Brigham and Women's Hospital
Boston, Massachusetts

Stuart H. Chen, MD
Clinical Fellow in Medicine
Beth Israel Deaconess Medical Center
Boston, Massachusetts

Aaron M. Cheng, MD
Assistant Professor
Division of Cardiothoracic Surgery
University of Washington
Seattle, Washington

Victor Chien, MD
Research Fellow in Surgery
Harvard Medical School
Beth Israel Deaconess Medical Center
Boston, Massachusetts

Alvin J. Chin, MD
Professor of Pediatrics, Emeritus
Perelman School of Medicine
University of Pennsylvania
Philadelphia, Pennsylvania

Cynthia S. Chin, MD
Director of the Women's Cancer Program Services
Thoracic Surgery
White Plains Hospital
White Plains, New York

Peter Chiu, MD
Resident, Department of Cardiothoracic Surgery
Stanford University School of Medicine
Stanford, California

Joseph C. Cleveland, Jr., MD
Professor of Cardiothoracic Surgery
Surgical Director, Cardiac Transplantation and MCS
University of Colorado Anschutz Medical Center
Aurora, Colorado

Lawrence H. Cohn, MD
Hubbard Professor of Cardiac Surgery
Harvard Medical School
Department of Surgery
Division of Cardiac Surgery
Brigham and Women's Hospital
Boston, Massachusetts

William E. Cohn, MD
Professor of Surgery
Michael E. DeBakey Department of Surgery
Baylor College of Medicine
Director, Center for Technology and Innovation
Director, Cullen Cardiovascular Research Laboratory
Texas Heart Institute
Houston, Texas

Yolonda L. Colson, MD, PhD
Professor
Department of Surgery
Harvard Medical School
Brigham and Women's Hospital
Boston, Massachusetts

Wilson S. Colucci, MD
Thomas J. Ryan Professor of Medicine
Professor of Physiology
Boston University School of Medicine
Chief, Section of Cardiovascular Medicine
Co-Director, Cardiovascular Center
Boston Medical Center
Boston, Massachusetts

Andrew C. Cook, PhD
Senior Lecturer
Cardiac Unit
UCL Institute of Cardiovascular Science
Great Ormond Street Hospital
NHS Foundation Trust
London, United Kingdom

Joseph S. Coselli, MD
Professor and Chief
Division of Cardiothoracic Surgery
Michael E. DeBakey Department of Surgery
Baylor College of Medicine
Chief, Section of Adult Cardiac Surgery
The Texas Heart Institute
Houston, Texas

Todd C. Crawford, MD
Division of Thoracic Surgery
The Johns Hopkins Medical Institutions
Baltimore, Maryland

Melissa Culligan, BSN, RN
Department of Thoracic Surgery
University of Pennsylvania Health System–Presbyterian
Philadelphia, Pennsylvania

François Dagenais, MD, FRCSC
Institut Universitaire de Cardiologie et de Pneumologie de Québec
Québec City, Québec, Canada

Ralph J. Damiano, Jr., MD
Evarts A. Graham Professor of Surgery
Chief, Division of Cardiothoracic Surgery
Washington University School of Medicine
Barnes-Jewish Hospital
St. Louis, Missouri

Thomas A. D'Amico, MD
Gary Hock Endowed Professor and Vice Chair of Surgery
Duke University School of Medicine
Chief, Section of General Thoracic Surgery
Program Director, Thoracic Surgery
Duke University Medical Center
Durham, North Carolina

Philippe G. Dartevelle, MD
Head, Service de Chirurgie Thoracique, Vasculaire et Transplantation Cardiopulmonaire
Hôpital Marie Lannelongue
Le Plessis Robinson, France

Tirone E. David, MD
Professor of Surgery
University of Toronto
Attending Surgeon
Peter Munk Cardiac Centre
Toronto General Hospital
Toronto, Ontario, Canada

Jonathan D'Cunha, MD, PhD
Associate Professor of Surgery
Vice Chairman, Academic Affairs and Education
Surgical Director, Lung Transplantation
Associate Program Director, Thoracic Surgery
Department of Cardiothoracic Surgery
University of Pittsburgh
Pittsburgh, Pennsylvania

Kim I. de la Cruz, MD
Assistant Professor of Cardiothoracic Surgery
Michael E. DeBakey Department of Surgery
Baylor College of Medicine
Clinical Staff
The Texas Heart Institute
Houston, Texas

Joseph A. Dearani, MD
Professor of Surgery
Chair, Cardiac Surgery
Division of Cardiovascular Surgery
Mayo Clinic
Rochester, Minnesota

Daniel T. DeArmond, MD
Cardiothoracic Surgery
University of Texas Health Science Center
San Antonio, Texas

Pedro J. del Nido, MD
William E. Ladd Professor of Surgery
Harvard Medical School
Chairman, Department of Cardiac Surgery
Boston Children's Hospital
Boston, Massachusetts

Tom R. DeMeester, MD
Professor and Chairman, Emeritus
Department of Surgery
University of Southern California
Los Angeles, California

Philippe Demers, MD, MSC, FRCSC
Associate Professor of Surgery
Cardiac Surgery
University of Montreal
Cardiovascular Surgeon
Montreal Heart Institute
Montreal, Quebec, Canada

Todd L. Demmy, MD
Chairman, Department of Thoracic Surgery
Roswell Park Cancer Institute
Buffalo, New York

Elisabeth U. Dexter, MD
Assistant Professor of Oncology
Department of Thoracic Surgery
Roswell Park Cancer Institute
Assistant Professor of Surgery
SUNY University at Buffalo
Buffalo, New York

Rajeev Dhupar, MD
Assistant Professor of Surgery
Department of Cardiothoracic Surgery
Division of Thoracic and Foregut Surgery
University of Pittsburgh Medical Center
Pittsburgh, Pennsylvania

James A. DiNardo, MD
Professor of Anesthesia
Boston Children's Hospital
Harvard Medical School
Boston, Massachusetts

Thomas P. Doyle, MD
Associate Professor of Pediatrics
Division of Cardiology
Vanderbilt University School of Medicine
Nashville, Tennessee

Afshin Ehsan, MD
Assistant Professor of Surgery
Brown Alpert Medical School
Rhode Island Hospital
Providence, Rhode Island

Gebrine El Khoury, MD, PhD
Professor
Department of Cardiovascular and Thoracic Surgery
Cliniques Universitaires Saint-Luc
Brussels, Belgium

Ethan R. Ellis, MD
Harvard-Thorndike Electrophysiology Institute
Cardiovascular Division
Harvard Medical School
Beth Israel Deaconess Medical Center
Boston, Massachusetts

Nassrene Y. Elmadhun, MD
Research Fellow
Cardiovascular Research Center
Warren Alpert Medical School
Brown University
Providence, Rhode Island
Surgical Resident
Beth Israel Deaconess Medical Center
Boston, Massachusetts

Sitaram M. Emani, MD
Assistant Professor in Surgery
Harvard Medical School
Assistant in Cardiac Surgery
Surgical Director, Adult Congenital Heart Program
Director, Complex Biventricular Repair Program
Surgical Director, Division of Cardiovascular Critical Care
Boston Children's Hospital
Boston, Massachusetts

Jeremy J. Erasmus, MD
Professor
Department of Diagnostic Imaging
The University of Texas MD Anderson Cancer Center
Houston, Texas

Dario O. Fauza, MD
Associate Professor of Surgery
Harvard Medical School
Associate in Surgery
Boston Children's Hospital
Boston, Massachusetts

Adam S. Fein, MD
Cardiac Services
Beth Israel Deaconess Medical Center
Boston, Massachusetts

Amy G. Fiedler, MD
Clinical Fellow in Surgery
Department of Surgery
Division of Cardiac Surgery
Brigham and Women's Hospital
Boston, Massachusetts

Murilo Foppa, MD, DSc
Department of Medicine
Cardiovascular Division
Harvard-Thorndike Laboratory
Harvard Medical School
Beth Israel Deaconess Medical Center
Boston, Massachusetts;
Division of Cardiology
Hospital de Clinicas de Porto Alegre
Federal University of Rio Grande do Sul
Brazil

Rosario V. Freeman, MD, MS
Medical Director, Echocardiography
Program Director, Cardiology Fellowship Programs
University of Washington
Seattle, Washington

Joseph Friedberg, MD, FACS
Chief of Thoracic Surgery
University of Pennsylvania Health System–Presbyterian
Philadelphia, Pennsylvania

Michael Friscia, MD
Associate, Thoracic and Cardiac Surgery
Geisinger Health System
Danville, Pennsylvania

Francis Fynn-Thompson, MD
Assistant Professor of Surgery
Surgical Director, Heart and Lung Transplantation
Surgical Director, Mechanical Circulatory Support Program
Program Director, Congenital Cardiac Surgery Residency/Fellowship
Department of Cardiac Surgery
Boston Children's Hospital
Harvard Medical School
Boston, Massachusetts

J. William Gaynor, MD
Professor of Surgery
Perelman School of Medicine
University of Pennsylvania
Attending Surgeon
Director, Fetal Neuroprotection and Neuroplasticity Program
Daniel M. Tabas Endowed Chair, Pediatric Cardiothoracic Surgery
The Children's Hospital of Philadelphia
Philadelphia, Pennsylvania

Liang Ge, PhD
Assistant Professor of Surgery
Department of Surgery
University of California, San Francisco School of Medicine
Department of Surgery
San Francisco VA Medical Center
San Francisco, California

Tal Geva, MD
Professor of Pediatrics
Harvard Medical School
Chief, Division of Noninvasive Cardiac Imaging
Senior Associate, Department of Cardiology
Boston Children's Hospital
Boston, Massachusetts

Neil M. Gheewala, MD
Cardiovascular Institute
Warren Alpert Medical School of Brown University
Providence, Rhode Island

A. Marc Gillinov, MD
The Judith Dion Pyle Chair in Heart Valve Research
Department of Thoracic and Cardiovascular Surgery
Cleveland Clinic
Cleveland, Ohio

Donald D. Glower, MD
Professor of Surgery
Department of Surgery
Division of Cardiovascular and Thoracic Surgery
Duke University School of Medicine
Durham, North Carolina

Andrew B. Goldstone, MD
Postdoctoral Research Fellow
Department of Cardiothoracic Surgery
Stanford University School of Medicine
Stanford, California

Shawn S. Groth, MD, MS
Assistant Professor of Surgery
Division of General Thoracic Surgery
Baylor College of Medicine
Houston, Texas

Frederick L. Grover, MD
Professor of Cardiothoracic Surgery
University of Colorado Anschutz Medical Center
Aurora, Colorado

Julius Guccione, PhD
Professor of Surgery
Department of Surgery
University of California, San Francisco School of Medicine
Associate Professor of Surgery
San Francisco VA Medical Center
San Francisco, California

Richard Ha, MD
Clinical Assistant Professor
Surgical Director, Mechanical Circulatory Support Program
Department of Cardiothoracic Surgery
Stanford University School of Medicine
Stanford, California

John W. Hammon, MD
Wake Forest University Baptist Medical Center
Winston-Salem, North Carolina

Jennifer M. Hanna, MD
Resident, General Surgery
Duke University School of Medicine
Durham, North Carolina

David G. Harrison, MD
Betty and Jack Bailey Professor of Medicine and Pharmacology
Director, Division of Clinical Pharmacology
Director, Center for Vascular Biology
Vanderbilt University Medical Center
Nashville, Tennessee

Thomas H. Hauser, MD, MMSc, MPH
Department of Medicine
Cardiovascular Division
Harvard-Thorndike Laboratory
Harvard Medical School
Beth Israel Deaconess Medical Center
Boston, Massachusetts

Matthew C. Henn, MD
Resident, Division of Cardiothoracic Surgery
Washington University School of Medicine
Barnes-Jewish Hospital
St. Louis, Missouri

Jennifer C. Hirsch-Romano, MD
Assistant Professor of Cardiac Surgery
University of Michigan
Ann Arbor, Michigan

Chuong D. Hoang, MD
Assistant Professor
Department of Cardiothoracic Surgery
Division of Thoracic Surgery
Stanford University School of Medicine
Stanford, California

Wayne L. Hofstetter, MD
Professor of Surgery
Director of Esophageal Surgery
Department of Thoracic and Cardiovascular Surgery
The University of Texas MD Anderson Cancer Center
Houston, Texas

Osami Honjo, MD, PhD
Cardiovascular Surgery
The Hospital for Sick Children
Toronto, Ontario, Canada

Tam T. Huynh, MD
Professor
Department of Thoracic and Cardiovascular Surgery
The University of Texas MD Anderson Cancer Center
Houston, Texas

Carlos E. Bravo Iñiguez, MD
Postdoctoral Fellow
Division of Thoracic Surgery
Brigham and Women's Hospital
Harvard Medical School
Boston, Massachusetts

Sebastian Iturra, MD
Structural Heart and Valve Center
Division of Cardiothoracic Surgery
Joseph B. Whitehead Department of Surgery
Emory University School of Medicine
Atlanta, Georgia

Jeffrey P. Jacobs, MD, FACS, FACC, FCCP
Professor of Surgery
Division of Cardiac Surgery
Department of Surgery
Johns Hopkins University
Baltimore, Maryland;
Chief, Division of Cardiovascular Surgery
Director, Andrews/Daicoff Cardiovascular Program
Surgical Director of Heart Transplantation and Extracorporeal Life Support Programs
Johns Hopkins All Children's Heart Institute
All Children's Hospital and Florida Hospital for Children
Saint Petersburg, Tampa, and Orlando, Florida

Marshall L. Jacobs, MD
Division of Cardiac Surgery
Department of Surgery
Johns Hopkins University
Baltimore, Maryland

Michael T. Jaklitsch, MD
Associate Professor
Surgeon, Division of Thoracic Surgery
Brigham & Women's Hospital
Harvard Medical School
Boston, Massachusetts

Stuart W. Jamieson, MB, FRCS
Distinguished Professor of Surgery
Endowed Chair, Division of Cardiothoracic Surgery
University of California, San Diego
San Diego, California

Doraid Jarrar, MD
Thoracic Surgeon
Einstein Healthcare
East Norriton, Pennsylvania

Craig M. Jarrett, MD
Department of Thoracic and Cardiovascular Surgery
Cleveland Clinic
Cleveland, Ohio

David R. Jones, MD
Professor and Chief of Thoracic Surgery
Memorial Sloan-Kettering Cancer Center
New York, New York

Mark E. Josephson, MD
Harvard-Thorndike Electrophysiology Institute, Cardiovascular Division
Harvard Medical School
Beth Israel Deaconess Medical Center
Boston, Massachusetts

Lilian P. Joventino, MD
Wentworth Health Partners Cardiovascular Group
Dover, New Hampshire

Amy L. Juraszek, MD
Associate Professor
Departments of Pediatrics and Pathology
University of Texas Southwestern Medical Center
Dallas, Texas

Stefan S. Kachala, MD
Department of Thoracic and Cardiovascular Surgery
Cleveland Clinic
Cleveland, Ohio

Larry R. Kaiser, MD
Dean and Professor of Surgery
Temple University School of Medicine
President and CEO
Temple University Health System
Sr. Executive Vice President for the Health Sciences
Temple University
Philadelphia, Pennsylvania

Kirk R. Kanter, MD
Professor of Surgery
Pediatric Cardiac Surgery
Emory University School of Medicine
Atlanta, Georgia

John M. Karamichalis, MD
Clinical Instructor in Surgery
Department of Surgery
Division of Pediatric Cardiothoracic Surgery
University of California, San Francisco
San Francisco, California

Aditya K. Kaza, MD
Assistant Professor of Surgery
Harvard Medical School
Associate in Cardiac Surgery
Department of Cardiac Surgery
Boston Children's Hospital
Boston, Massachusetts

Clinton D. Kemp, MD
Division of Thoracic Surgery
The Johns Hopkins Medical Institutions
Baltimore, Maryland

Kemp H. Kernstine, Sr., MD, PhD
Professor and Chief, Division of Thoracic Surgery
Department of Cardiovascular & Thoracic Surgery
University of Texas Southwestern Medical Center
Dallas, Texas

Suresh Keshavamurthy, MD
Cleveland Clinic
Cleveland, Ohio

Shaf Keshavjee, MD, MSc, FRCSC, FACS
Surgeon-in-Chief, University Health Network
James Wallace McCutcheon Chair in Surgery
Professor, Division of Thoracic Surgery
University of Toronto
Toronto, Ontario, Canada

Deborah J. Kozik, DO
Assistant Professor of Surgery
Department of Cardiovascular and Thoracic Surgery
University of Louisville
Cardiothoracic Surgery
Kosair Children's Hospital
Louisville, Kentucky

Roger J. Laham, MD
Associate Professor of Medicine
Harvard Medical School
Research Investigator
CardioVascular Institute
Beth Israel Deaconess Medical Center
Boston, Massachusetts

Michael J. Landzberg, MD
Director, Boston Adult Congenital Heart (BACH) and Pulmonary Hypertension Program
Department of Cardiology
Brigham and Women's Hospital and Boston Children's Hospital
Boston, Massachusetts

Christopher P. Lawrance, MD
Resident, Division of Cardiothoracic Surgery
Washington University School of Medicine
Barnes-Jewish Hospital
St. Louis, Missouri

Lawrence S. Lee, MD
Clinical Fellow in Surgery
Harvard Medical School
Department of Surgery
Division of Cardiac Surgery
Brigham and Women's Hospital
Boston, Massachusetts

Scott A. LeMaire, MD
Professor and Vice Chair for Research
Michael E. DeBakey Department of Surgery
Baylor College of Medicine
Professional Staff, Department of Cardiovascular Surgery
The Texas Heart Institute
Houston, Texas

Sidney Levitsky, MD
David W. and David Cheever Professor of Surgery
Harvard Medical School
Director, Cardiothoracic Surgery Care Group
Senior Vice Chairman, Department of Surgery
Beth Israel Deaconess Medical Center
Boston, Massachusetts

Jerrold H. Levy, MD, FAHA, FCCM
Professor of Anesthesiology
Associate Professor of Surgery
Departments of Anesthesiology, Surgery, and Critical Care
Co-Director, Cardiothoracic ICU
Duke University School of Medicine
Duke University Medical Center
Durham, North Carolina

Philip A. Linden, MD
Associate Professor of Surgery
Case Western Reserve School of Medicine
Chief, Division of Thoracic and Esophageal Surgery
University Hospitals Case Medical Center
Cleveland, Ohio

Michael J. Liptay, MD
The Mary and John Bent Professor and Chairperson
Department of Cardiovascular and Thoracic Surgery
Rush University Medical Center
Chicago, Illinois

Virginia R. Litle, MD, FACS
Associate Professor of Surgery
Department of Surgery
Division of Thoracic Surgery
Boston University School of Medicine
Boston, Massachusetts

Mauro Lo Rito, MD
Cardiovascular Surgery
The Hospital for Sick Children
Toronto, Ontario, Canada

James D. Luketich, MD
Henry T. Bahnson Professor and Chairman
Department of Cardiothoracic Surgery
Chief, Division of Thoracic and Foregut Surgery
University of Pittsburgh School of Medicine
Director, Thoracic Surgical Oncology
Co-Director, Lung Cancer Center
University of Pittsburgh Medical Center
Pittsburgh, Pennsylvania

Bruce W. Lytle, MD
Chairman, Strategic Development and Planning for Cardiovascular Medicine and Surgery
The Heart Hospital Baylor Plano
Plano, Texas

Michael Madani, MD
Professor of Surgery
Chief, Division of Cardiothoracic Surgery
University of California, San Diego
San Diego, California

Feroze Mahmood, MD
Associate Professor of Anaesthesiology
Harvard Medical School
Director, Vascular Anesthesia/Perioperative Echocardiography
Beth Israel Deaconess Medical Center
Harvard Medical Faculty Physicians at Beth Israel Deaconess Medical Center
Boston, Massachusetts

Hari R. Mallidi, MD
Associate Professor of Surgery
Chief, Division of Transplant & Assist Devices
Lester and Sue Smith Endowed Chair in Surgery
Baylor College of Medicine
Houston, Texas

Abeel A. Mangi, MD
Associate Professor of Surgery, Section of Cardiac Surgery
Surgical Director, Center for Advanced Heart Failure, Mechanical Circulatory Support and Heart Transplantation
Surgical Director, Trans-Catheter Therapies
Yale University
New Haven, Connecticut

Warren J. Manning, MD
Departments of Medicine and Radiology
Cardiovascular Division
Harvard-Thorndike Laboratory
Harvard Medical School
Beth Israel Deaconess Medical Center
Boston, Massachusetts

Edith M. Marom, MD
Professor
Department of Diagnostic Imaging
The University of Texas MD Anderson Cancer Center
Houston, Texas

Audrey C. Marshall, MD
Chief, Invasive Cardiology
Boston Children's Hospital
Boston, Massachusetts

Mauricio Perez Martinez, MD
Division of Thoracic Surgery
Brigham and Women's Hospital
Harvard Medical School
Boston, Massachusetts

Christopher E. Mascio, MD
Assistant Professor of Clinical Medicine
Perelman School of Medicine
University of Pennsylvania
Pediatric Cardiothoracic Surgeon
Division of Cardiothoracic Surgery
The Children's Hospital of Philadelphia
Philadelphia, Pennsylvania

David P. Mason, MD
Chief, Thoracic Surgery and Lung Transplantation
Department of Thoracic Surgery
Baylor University Medical Center
Dallas, Texas

Douglas J. Mathisen, MD
Chief of Thoracic Surgery
Massachusetts General Hospital
Boston, Massachusetts

Kenneth L. Mattox, MD, FACS
Professor of Surgery
Division of Cardiothoracic Surgery
Michael E. DeBakey Department of Surgery
Baylor College of Medicine
Houston, Texas

Robina Matyal, MD
Associate Professor of Anaesthesiology
Harvard Medical School
Beth Israel Deaconess Medical Center
Boston, Massachusetts

James D. McCully, PhD
Associate Professor of Surgery
Harvard Medical School
Department of Cardiac Surgery
Boston Children's Hospital
Boston, Massachusetts

Robert J. McKenna, Jr., MD
Director, Thoracic Surgery
Surgery
Cedars-Sinai Medical Center
Los Angeles, California

Ciaran McNamee, MD
Instructor in Surgery
Harvard Medical School
Associate Surgeon
Brigham and Women's Hospital
Boston, Massachusetts

Jeffrey D. McNeil, MD
Colonel, U.S. Air Force
Chief, Cardiothoracic Surgery Service
San Antonio Military Medical Center
San Antonio, Texas
Clinical Assistant Professor, Cardiothoracic Surgery
University of Texas Health Science Center, San Antonio
San Antonio, Texas

Lorenzo Menicanti, MD
Chief of Cardiac Surgery
IRCCS Policlinico San Donato
Milan, Italy

Carlos A. Mestres, MD, PhD, FETCS
Senior Consultant
Department of Cardiovascular Surgery
Hospital Clinico
University of Barcelona
Barcelona, Spain;
Cardiothoracic and Vascular Surgery
Heart and Vascular Institute
Cleveland Clinic Abu Dhabi
Abu Dhabi, United Arab Emirates

Bret A. Mettler, MD
Assistant Professor
Division of Pediatric Cardiac Surgery
Vanderbilt University School of Medicine
Department of Cardiac Surgery
Vanderbilt University Medical Center
Nashville, Tennessee

Bryan Fitch Meyers, MD, MPH
Patrick and Joy Williamson Professor of Surgery
Chief, Thoracic Surgery
Washington University School of Medicine
St. Louis, Missouri

Stephanie Mick, MD
Cardiovascular Surgeon
Department of Thoracic and Cardiovascular Surgery
Cleveland Clinic
Cleveland, Ohio

Tomislav Mihaljevic, MD
Chief of Staff and Chairman of the Heart and Vascular Institute
Cleveland Clinic Abu Dhabi
Abu Dhabi, United Arab Emirates;
Attending Surgeon
Department of Thoracic and Cardiovascular Surgery
Cleveland Clinic
Professor of Surgery
Cleveland Clinic Lerner College of Medicine at Case Western University
Cleveland, Ohio

Carmelo A. Milano, MD
Professor of Surgery
Cardiovascular and Thoracic Surgery
Duke University
Durham, North Carolina

D. Craig Miller, MD
Thelma and Henry Doelger Professor of Cardiovascular Surgery
Department of Cardiovascular Surgery
Stanford University School of Medicine
Department of Cardiothoracic Surgery
Stanford University Medical Center
Stanford, California

Daniel L. Miller, MD, FACS
Clinical Professor of Surgery
Georgia Regents University
Chief, General Thoracic Surgery
WellStar Health System
Mayo Clinic Care Network
Marietta, Georgia

Meagan M. Miller, RN, BSN
Vanderbilt University Medical Center
Nashville, Tennessee

John D. Mitchell, MD
Courtenay C. and Lucy Patten Davis Endowed Chair in Thoracic Surgery
Professor and Chief, Section of General Thoracic Surgery
Division of Cardiothoracic Surgery
University of Colorado School of Medicine
Aurora, Colorado

Mario Montealegre-Gallegos, MD
Department of Anaesthesia
Harvard Medical School
Beth Israel Deaconess Medical Center
Boston, Massachusetts

Neal G. Moores, MD
Department of Thoracic and Cardiovascular Surgery
Cleveland Clinic
Cleveland, Ohio

Charles E. Murphy, MD
Assistant Professor of Surgery
Division of Cardiovascular and Thoracic Surgery
Duke University School of Medicine
Duke University Medical Center
Durham, North Carolina

Raghav A. Murthy, MD
Department of Cardiovascular & Thoracic Surgery
University of Texas Southwestern Medical Center
Dallas, Texas

Sudish C. Murthy, MD, PhD
Section Head, General Thoracic Surgery
Surgical Director, Center for Major Airway Disease
Department of Thoracic and Cardiovascular Surgery
Cleveland Clinic
Cleveland, Ohio

Sacha Mussot, MD
Hôpital Marie Lannelongue
Service de Chirurgie Thoracique, Vasculaire et Transplantation Cardiopulmonaire
Le Plessis Robinson, France

Yoshifumi Naka, MD, PhD
Professor of Surgery
Columbia University College of Physicians and Surgeons
Attending Surgeon
New York–Presbyterian Hospital
New York, New York

Meena Nathan, MD, FRCS
Instructor in Surgery
Harvard Medical School
Staff Cardiac Surgeon
Department of Cardiac Surgery
Boston Children's Hospital
Boston, Massachusetts

Kurt D. Newman, MD
President and Chief Executive Officer
Children's National Medical Center
Washington, DC

Chukwumere Nwogu, MD
Associate Professor
Department of Thoracic Surgery
Roswell Park Cancer Institute
Buffalo, New York

Kirsten C. Odegard, MD
Associate Professor
Department of Anesthesiology, Perioperative and Pain Medicine
Boston Children's Hospital
Boston, Massachusetts

Daniel S. Oh, MD
Assistant Professor of Surgery
Division of Thoracic Surgery
University of Southern California
Los Angeles, California

Richard G. Ohye, MD
Professor of Cardiac Surgery
University of Michigan
Ann Arbor, Michigan

Mark W. Onaitis, MD
Associate Professor of Surgery
Department of Surgery
Division of Cardiovascular and Thoracic Surgery
Duke University School of Medicine
Duke University Medical Center
Durham, North Carolina

Aleksandra Ostojic, MSc
Division of Cardiac Surgery
University of Ottawa Heart Institute
Department of Cellular and Molecular Medicine
University of Ottawa
Ottawa, Ontario, Canada

Harald C. Ott, MD
Division of Thoracic Surgery
Massachusetts General Hospital
Boston, Massachusetts

Maral Ouzounian, MD, PhD
Assistant Professor of Surgery
University of Toronto
Cardiovascular Surgeon
Division of Cardiovascular Surgery
University Health Network
Toronto General Hospital
Toronto, Ontario, Canada

Khurram Owais, MD
Department of Anaesthesia
Harvard Medical School
Beth Israel Deaconess Medical Center
Boston, Massachusetts

Massimo Padalino, MD, PhD
Department of Cardio Thoracic and Vascular Sciences
University Hospital
Padova, Italy

Konstantinos Papadakis, MD
Instructor in Surgery
Harvard Medical School
Department of Surgery
Boston Children's Hospital
Boston, Massachusetts

G. A. Patterson, MD
Evarts A. Graham Professor of Surgery
Chief, Division of Cardiothoracic Surgery
Washington University
St. Louis, Missouri

Edward F. Patz, Jr., MD
Professor
Department of Radiology
Duke University
Durham, North Carolina

Subroto Paul, MD
Associate Professor
Department of Cardiothoracic Surgery
Weill Cornell Medical College
New York, New York

Arjun Pennathur, MD
Sampson Family Endowed Chair in Thoracic Surgical Oncology
Associate Professor of Cardiothoracic Surgery
Department of Cardiothoracic Surgery
University of Pittsburgh School of Medicine
University of Pittsburgh Medical Center
Pittsburgh, Pennsylvania

Yaron Perry, MD
Clinical Associate Professor of Surgery
Case Western Reserve University School of Medicine
Director, Minimally Invasive Esophageal Surgery
University Hospitals Case Medical Center
Cleveland, Ohio

Robert N. Piana, MD
Professor of Medicine
Division of Cardiovascular Medicine
Director, Adult Congenital Interventional Program
Vanderbilt University Medical Center
Nashville, Tennessee

Frank A. Pigula, MD
Associate Professor of Surgery
Harvard Medical School
Senior Associate in Cardiac Surgery
Clinical Director, Cardiac Surgery Program
Director, Neonatal Cardiac Surgery Program
Boston Children's Hospital
Boston, Massachusetts

Duane S. Pinto, MD, MPH
Associate Professor of Medicine
Harvard Medical School
Associate Director, Cardiac Catheterization Laboratory
Beth Israel Deaconess Medical Center
Boston, Massachusetts

Jose L. Pomar, MD, PhD, FETCS
Senior Consultant and Professor of Surgery
Department of Cardiovascular Surgery
Hospital Clinico
University of Barcelona
Barcelona, Spain

Ourania Preventza, MD
Assistant Professor of Cardiothoracic Surgery
Michael E. DeBakey Department of Surgery
Baylor College of Medicine
Clinical Staff
The Texas Heart Institute
Houston, Texas

Bradley Pua, MD
Assistant Professor of Radiology
Weill Cornell Medical College
Program Director, Interventional Radiology Fellowship
Director, Lung Cancer Screening Program
New York Presbyterian Hospital/Weill Cornell Medical Center
New York, New York

Varun Puri, MD
Assistant Professor of Surgery
Division of Cardiothoracic Surgery
Washington University
St. Louis, Missouri

Luis Quinonez, MD
Instructor in Surgery
Harvard Medical School
Assistant in Cardiac Surgery
Department of Cardiac Surgery
Boston Children's Hospital
Boston, Massachusetts

Siva Raja, MD, PhD
Department of Thoracic and Cardiovascular Surgery
Cleveland Clinic
Cleveland, Ohio

Mark Ratcliffe, MD
Professor of Surgery
Department of Surgery
University of California, San Francisco
Chief Surgical Consultant
Sierra Pacific VA Network
San Francisco, California

Michael J. Reardon, MD
Professor of Cardiothoracic Surgery
Allison Family Distinguished Chair of Cardiovascular Research
Houston Methodist DeBakey Heart & Vascular Center
Houston, Texas

John J. Reilly, Jr., MD
Dean
University of Colorado School of Medicine
Vice Chancellor for Health Affairs
University of Colorado
Aurora, Colorado

Karl G. Reyes, MD
Department of Thoracic and Cardiovascular Surgery
Cleveland Clinic
Cleveland, Ohio

Thomas W. Rice, MD
Head, Section of General Thoracic Surgery
Department of Thoracic and Cardiovascular Surgery
Heart and Vascular Institute
Cleveland Clinic
Cleveland, Ohio

Robert C. Robbins, MD
President and Chief Executive Officer
Texas Medical Center
Houston, Texas;
Consulting Professor
Stanford Cardiovascular Institute
Stanford, California

Gaetano Rocco, MD, FRCS(Ed), FECTS
Director, Department of Thoracic Surgery and Oncology
National Cancer Institute, Pascale Foundation
Naples, Italy

Fraser D. Rubens, MD, MSc, FACS, FRCSC
Professor of Surgery
Division of Cardiac Surgery
Residency Program Director
University of Ottawa Heart Institute
Ottawa, Ontario, Canada

Marc Ruel, MD, MPH
Professor and Chair
Division of Cardiac Surgery
University of Ottawa Heart Institute
Ottawa, Ontario, Canada

Valerie W. Rusch, MD
Attending Surgeon, Thoracic Service
Vice Chair for Clinical Research
Miner Family Chair in Intrathoracic Cancers
Department of Surgery
Memorial Sloan-Kettering Cancer Center
New York, New York

Ashraf A. Sabe, MD
Clinical Teaching Fellow, General Surgery
Harvard Medical School
Resident, General Surgery
Beth Israel Deaconess Medical Center
Boston, Massachusetts;
Research Fellow, Cardiothoracic Surgery
Warren Alpert Medical School of Brown University
Providence, Rhode Island

Sameh M. Said, MD
Senior Associate Consultant
Division of Cardiovascular Surgery
Mayo Clinic
Rochester, Minnesota

Pamela P. Samson, MD, MPHS
Resident, Department of Surgery
Washington University and Barnes-Jewish Hospital
St. Louis, Missouri

Stephen P. Sanders, MD
Professor of Pediatrics
Harvard Medical School
Director, Cardiac Registry
Departments of Cardiology, Pathology, Cardiac Surgery
Boston Children's Hospital
Boston, Massachusetts

Eric L. Sarin, MD
Assistant Professor of Surgery
Structural Heart and Valve Center
Division of Cardiothoracic Surgery
Joseph B. Whitehead Department of Surgery
Emory University School of Medicine
Atlanta, Georgia

Hartzell V. Schaff, MD
Professor of Surgery
Mayo Clinic
Rochester, Minnesota

Lara W. Schaheen, MD
Resident, Department of Cardiothoracic Surgery
University of Pittsburgh School of Medicine
Pittsburgh, Pennsylvania

Christopher W. Seder, MD
Assistant Professor of Thoracic and Cardiac Surgery
Rush University Medical Center
Chicago, Illinois

Frank W. Sellke, MD
Karl Karlson & Gloria Karlson Professor and Chief of Cardiothoracic Surgery
Warren Alpert Medical School of Brown University and Rhode Island Hospital
Director, Lifespan Cardiovascular Institute
Providence, Rhode Island

Boris Sepesi, MD
Assistant Professor
Department of Thoracic and Cardiovascular Surgery
Division of Surgery
The University of Texas MD Anderson Cancer Center
Houston, Texas

Rohit Shahani, MD
Cardiothoracic Surgery
Hudson Cardiothoracic Surgeons
Poughkeepsie, New York

Robert C. Shamberger, MD
Robert E. Gross Professor of Surgery
Harvard Medical School
Chief of Surgery
Boston Children's Hospital
Boston, Massachusetts

Oz M. Shapira, MD
Professor and Chairman
Department of Cardiothoracic Surgery
Hebrew University
Hadassah Medical Center
Jerusalem, Israel

Steven S. Shay, MD
Department of Gastroenterology
Digestive Disease Institute
Cleveland Clinic
Cleveland, Ohio

Joseph B. Shrager, MD
Professor, Department of Cardiothoracic Surgery
Chief, Division of Thoracic Surgery
Stanford University School of Medicine
Stanford, California

Ming-Sing Si, MD
Assistant Professor of Cardiac Surgery
University of Michigan
Ann Arbor, Michigan

Steve K. Singh, MD, MSc, FRCSC
Assistant Professor of Surgery
Division of Transplant & Assist Devices
Baylor College of Medicine
Houston, Texas

Peter K. Smith, MD
Professor and Chief, Thoracic Surgery
Duke University
Durham, North Carolina

Neel R. Sodha, MD
Assistant Professor of Surgery
Cardiothoracic Surgery
Warren Alpert Medical School of Brown University
Providence, Rhode Island

R. John Solaro, PhD
Distinguished University Professor and Head
Department of Physiology and Biophysics
University of Illinois at Chicago College of Medicine
Chicago, Illinois

Harmik J. Soukiasian, MD
Associate Director, Thoracic Surgery
Cedars-Sinai Medical Center
Los Angeles, California

David Spurlock, MD
Junior Fellow, Cardiac Surgery
University of Michigan
Ann Arbor, Michigan

Giovanni Stellin, MD
Director of Pediatric and Congenital Cardiac Surgery
Department of Cardio Thoracic and Vascular Sciences
University Hospital
Padova, Italy

Brendon M. Stiles, MD
Associate Professor of Cardiothoracic Surgery
Weill Cornell Medical College
Cardiothoracic Surgery
New York Presbyterian Hospital/Weill Cornell Medical College
New York, New York

Michaela Straznicka, MD
Thoracic Surgeon
Sutter Health Medical Center
Walnut Creek, California

David A. Stump, PhD
Wake Forest University Baptist Medical Center
Winston-Salem, North Carolina

David J. Sugarbaker, MD
Director, The Lung Institute
Chief, Division of Thoracic Surgery
The Olga Keith Wiess Chair of Surgery
Baylor College of Medicine
Houston, Texas

Erik J. Suuronen, PhD
Division of Cardiac Surgery
University of Ottawa Heart Institute
Department of Cellular and Molecular Medicine
University of Ottawa
Ottawa, Ontario, Canada

Lars G. Svensson, MD, PhD
Professor of Surgery, Thoracic and Cardiovascular Surgery
Chairman, Heart and Vascular Institute
Cleveland Clinic
Cleveland, Ohio

Scott J. Swanson, MD
Director, Minimally Invasive Thoracic Surgery
Brigham and Women's Hospital
Vice Chair, Cancer Affairs
Department of Surgery, Brigham and Women's Hospital
Chief Surgical Officer
Dana-Farber Cancer Institute
Professor of Surgery
Harvard Medical School
Boston, Massachusetts

Wilson Y. Szeto, MD
Associate Professor of Surgery
Division of Cardiovascular Surgery
Department of Surgery
University of Pennsylvania
Philadelphia, Pennsylvania

Sharven Taghavi, MD
Resident, Department of Surgery
Temple University
Philadelphia, Pennsylvania

Hiroo Takayama, MD, PhD
Assistant Professor of Surgery
Columbia University College of Physicians and Surgeons
Attending Surgeon
New York–Presbyterian Hospital
New York, New York

Koji Takeda, MD, PhD
Assistant Professor of Surgery
Columbia University College of Physicians and Surgeons
Attending Surgeon
New York–Presbyterian Hospital
New York, New York

Ravi R. Thiagarajan, MBBS, MPH
Senior Associate in Cardiology
Associate Professor of Pediatrics
Boston Children's Hospital
Boston, Massachusetts

Patricia A. Thistlethwaite, MD, PhD
Professor of Surgery
Program Director, Division of Cardiothoracic Surgery
University of California, San Diego
San Diego, California

Vinod H. Thourani, MD
Professor of Surgery
Structural Heart and Valve Center
Division of Cardiothoracic Surgery
Joseph B. Whitehead Department of Surgery
Emory University School of Medicine
Atlanta, Georgia

Hadi D. Toeg, MD, MSc
Surgical Resident
Division of Cardiac Surgery
University of Ottawa Heart Institute
Ottawa, Ontario, Canada

Michael Z. Tong, MD, MBA
Associate Staff, Thoracic and Cardiovascular Surgery
Heart and Vascular Institute
Cleveland Clinic
Cleveland, Ohio

Alexander G. Truesdell, MD
Cardiac and Vascular Interventionalist
PinnacleHealth CardioVascular Institute
Harrisburg, Pennsylvania

Peter I. Tsai, MD, FACS
Assistant Professor of Surgery
Division of Cardiothoracic Surgery
Michael E. DeBakey Department of Surgery
Baylor College of Medicine
Houston, Texas

Harold C. Urschel, Jr., MD†
Professor of Cardiovascular and Thoracic Surgery
University of Texas Southwestern Medical School
Chair, Cardiovascular and Thoracic Surgical Research, Education, and Clinical Excellence
Department of Cardiovascular and Thoracic Surgery
Baylor University Medical Center
Dallas, Texas

†Deceased.

Anne Marie Valente, MD
Associate Professor of Pediatrics and Internal Medicine
Harvard Medical School
Outpatient Director, Boston Adult Congenital Heart Disease and Pulmonary Hypertension Program
Department of Cardiology
Boston Children's Hospital
Department of Medicine
Division of Cardiology
Brigham and Women's Hospital
Boston, Massachusetts

Prashanth Vallabhajosyula, MD, MS
Assistant Professor of Surgery
Division of Cardiovascular Surgery
Department of Surgery
University of Pennsylvania
Philadelphia, Pennsylvania

Jeffrey B. Velotta, MD
Thoracic Surgery
Oakland Medical Center
Oakland, California

Vladimiro Vida, MD, PhD
Department of Cardio Thoracic and Vascular Sciences
University Hospital
Padova, Italy

Gus J. Vlahakes, MD
Professor of Surgery
Harvard Medical School
Massachusetts General Hospital
Boston, Massachusetts

Pierre Voisine, MD, FRCSC
Department of Cardiac Surgery
Institut Universitaire de Cardiologie et de Pneumologie de Québec
Québec City, Québec, Canada

Matthew J. Wall, Jr., MD, FACS
Professor of Surgery
Division of Cardiothoracic Surgery
Michael E. DeBakey Department of Surgery
Baylor College of Medicine
Houston, Texas

Garrett L. Walsh, MD
Professor of Surgery
Department of Thoracic and Cardiovascular Surgery
Division of Surgery
The University of Texas MD Anderson Cancer Center
Houston, Texas

Dustin M. Walters, MD
Division of Cardiothoracic Surgery
University of Washington Medical Center
Seattle, Washington

Benjamin Wei, MD
Assistant Professor of Surgery
Division of Cardiothoracic Surgery
University of Alabama at Birmingham
Birmingham, Alabama

Ian J. Welsby, MB BS
Associate Professor of Anesthesiology
Departments of Anesthesiology, Surgery, and Critical Care
Duke University School of Medicine
Durham, North Carolina

Margaret V. Westfall, PhD
Associate Professor
Department of Cardiac Surgery
University of Michigan School of Medicine
Ann Arbor, Michigan

Daniel C. Wiener, MD
Assistant Professor of Surgery
Harvard Medical School
Thoracic Surgeon
Brigham and Women's Hospital
Boston, Massachusetts

Benson R. Wilcox, MD[†]
Professor of Surgery
Department of Cardiothoracic Surgery
University of North Carolina at Chapel Hill
University of North Carolina Hospital
Chapel Hill, North Carolina

Judson B. Williams, MD, MHS
Resident, Cardiothoracic Surgery
Duke University
Durham, North Carolina

Jay M. Wilson, MD
Associate Professor of Surgery
Harvard Medical School
Senior Associate in Surgery
Boston Children's Hospital
Boston, Massachusetts

Y. Joseph Woo, MD
Norman E. Shumway Professor and Chair
Department of Cardiothoracic Surgery
Stanford University School of Medicine
Professor, by courtesy, Department of Bioengineering
Stanford University
Stanford, California

Douglas E. Wood, MD
Professor and Chief, Endowed Chair in Lung Cancer Research
Division of Cardiothoracic Surgery
University of Washington
Seattle, Washington

John V. Wylie, Jr., MD
Tufts University School of Medicine
St. Elizabeth's Medical Center
Boston, Massachusetts

Stephen C. Yang, MD
Professor of Surgery
The Johns Hopkins Medical Institutions
Baltimore, Maryland

Sai Yendamuri, MD
Associate Professor
Department of Thoracic Surgery
Roswell Park Cancer Institute
Buffalo, New York

Susan B. Yeon, MD, JD
Department of Medicine
Cardiovascular Division
Harvard-Thorndike Laboratory
Harvard Medical School
Beth Israel Deaconess Medical Center
Boston, Massachusetts;
Deputy Editor
UpToDate
Wolters Kluwer Health
Waltham, Massachusetts

Peter J. Zimetbaum, MD
Associate Professor of Medicine
Harvard Medical School
Cardiac Services
Beth Israel Deaconess Medical Center
Boston, Massachusetts

[†]Deceased.

Preface

Since its beginning as a specialty to treat tuberculosis and empyema, thoracic surgery has undergone constant change. Indeed, much has evolved in the fields of adult and pediatric cardiovascular and thoracic surgery even since our last edition. Our new ninth edition contains the latest information on the diagnosis and treatment of disease of the thorax. Especially in such areas as repair of aortic and mitral valvular disease, intervention for congenital heart disease, minimally invasive thoracic and cardiac surgery, surgical treatment of arrhythmias, and endovascular treatment of aortic disease, the field has markedly transformed. As with the previous editions, many of the same authors were asked to update their chapters, but some chapters have been added or eliminated and many others have been completely rewritten. Often new authors were chosen not based on poorly written previous chapters but to provide a novel perspective. We hope that the ninth edition will be received with the same enthusiasm as the last.

Several years ago, we lost one of the former editors of this textbook and a giant in the field of surgery, Dr. David Sabiston. We are fortunate to still have with us another editor, Dr. Frank Spencer. Dr. Spencer is not only one of the true pioneers in our specialty but a great mentor to many in our field. We are all indebted to both Dr. Sabiston and Dr. Spencer for their innumerable contributions to the field of surgery.

Finally, we would like to thank our families for providing immeasurable support not only for this textbook but for our entire careers.

Frank W. Sellke
Pedro J. del Nido
Scott J. Swanson

Contents

VOLUME ONE

SECTION 1
THORACIC SURGERY

PART H
CHEST WALL, 398

PART I
PLEURA, 461

PART J
DIAPHRAGM, 525

PART K
ESOPHAGUS—BENIGN DISEASE, 574

PART L
ESOPHAGUS—CANCER, 644

PART M
MEDIASTINUM, 697

PART N
THE FUTURE, 751

SECTION 2
ADULT CARDIAC SURGERY

PART A
BASIC SCIENCE, 786

Video Contents

[1]From Coselli JS, LeMaire SA: Extent II repair of thoracoabdominal aortic aneurysm secondary to chronic dissection. *Ann Cardiothorac Surg* 1(3):394–397, 2012.
[2]Courtesy Ralph Chitwood, MD, Karen A. Gersch, MD, Michael W. Chu, MD, L. W. Nifong, MD, and Jerome Fuller, MD.
[3]From *Sabiston & Spencer Surgery of the Chest*, ed 8.
[4]From Vassiliades TA: Endoscopic and traditional minimally invasive direct coronary artery bypass. In Sellke FW, editor: *Atlas of cardiac surgical techniques*, Philadelphia, 2009, Elsevier.
[5]Courtesy Keith Horvath, MD.
[6]From Frazier OH: Implantation of the Heart Mate II. In Sellke FW, editor: *Atlas of cardiac surgical techniques*, Philadelphia, 2009, Elsevier.
[7]From Reitz BA, Baumgartner WA, Borkon AM, the American College of Surgeons Video-Based Education Collection.
[8]Courtesy Lorenzo Menicanti, MD, and Marisa Di Donato, MD.

This page intentionally left blank

SABISTON & SPENCER

SURGERY *of the* CHEST

This page intentionally left blank

SECTION 1

THORACIC SURGERY

SECTION OUTLINE

PART A

EVALUATION AND CARE

PART OUTLINE

CHAPTER 1

Anatomy of the Thorax

Cynthia S. Chin • Rohit Shahani

CHAPTER OUTLINE

The thorax is the upper part of the trunk, bounded by the diaphragm inferiorly, the thoracic inlet superiorly, and the thoracic cage between. Vital organs, such as the heart and lungs, reside completely within the thoracic cavity, and other, equally vital organs, such as the aorta and esophagus, extend into the abdominal cavity. The thorax can be divided into a right and left hemithorax, separated by the mediastinum. This chapter gives an overview of the anatomy of the thoracic cavity and its contents.

THORACIC CAGE

The cylindrical thoracic cage has two main purposes: it provides protection for the underlying organs, and the dynamic interactions of the bony and muscular components of the chest wall allow changes in respiratory volumes.

The bony thorax has two apertures, or openings: the superior thoracic aperture, often referred to as the thoracic inlet or cervicothoracic junction, and the inferior thoracic aperture (Fig. 1-1*A*).

Thoracic Inlet

The thoracic inlet is limited by the body of the first thoracic vertebra posteriorly, the first pair of ribs and their costal cartilages anterolaterally, and the superior border of the manubrium anteriorly. Many important structures travel through the cervicothoracic junction. Resection of malignancies (e.g., Pancoast tumor) or repair of thoracic outlet syndrome requires intimate knowledge of the anatomic relationships in this area. In this kidney-shaped inlet, the trachea is midline and behind the great vessels, and the esophagus is posterior and slightly to its left. The innominate artery arises from the aortic arch and passes posterior to the manubrium and anterior to the trachea as it travels cephalad. The right and left internal jugular and subclavian veins join behind their respective sternoclavicular joints to form the left and right brachiocephalic veins. The left brachiocephalic vein travels right to join its counterpart to form the superior vena cava. The main muscles of this region are the sternocleidomastoid and scalene muscles, and the main nerves form the brachial plexus, but the phrenic and vagus nerves also pass through this aperture.

As the margin of the aperture slopes inferoanteriorly, the apex of each lung and its covering pleura (pleural cupola) project superiorly through the lateral parts of the thoracic inlet and are covered by a piece of cervical fascia, the suprapleural membrane (Sibson fascia).

Cervicoaxillary Canal

The cervicoaxillary canal is bounded by the first rib inferiorly, the clavicle superiorly, and the costoclavicular ligament medially (Fig. 1-2). The structures that pass through this space include the subclavian vein and artery and the brachial plexus.

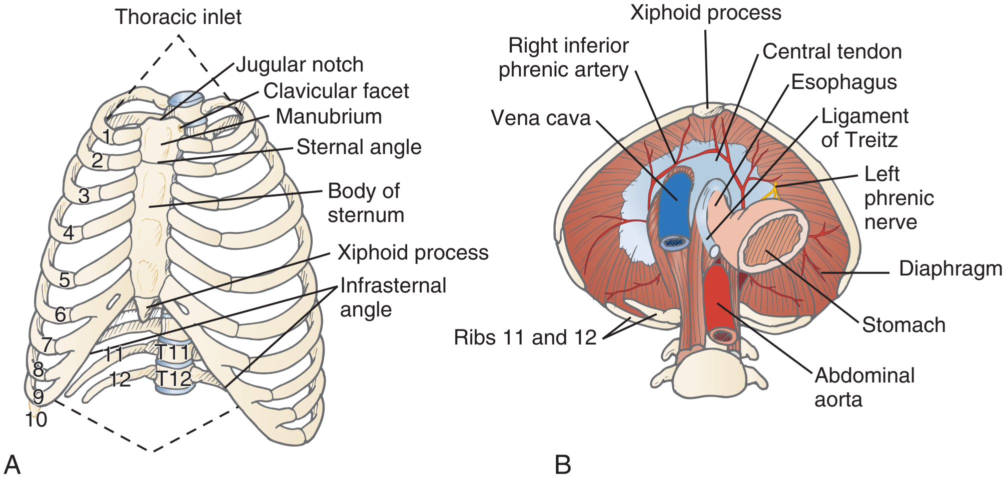

FIGURE 1-1 ■ **A,** Bony thorax. **B,** Inferior thoracic aperture. The vena cava enters the right hemithorax through the most cranial diaphragmatic opening, located at the level of the eighth thoracic vertebra (T8). The esophagus and vagus nerves enter the abdomen at the level of the T10 vertebra. The hiatus at T12 allows the aorta, azygos vein, and thoracic duct to pass in their respective directions.

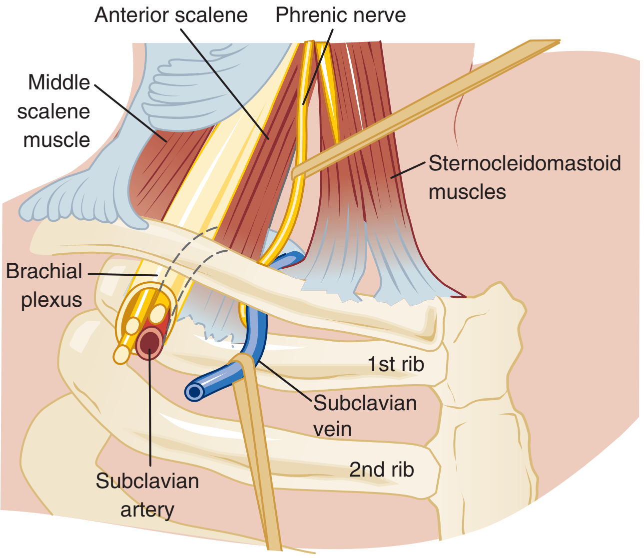

FIGURE 1-2 ■ Cervicoaxillary canal and the structures that traverse this opening.

The subclavian artery passes over the first rib and goes between the scalenus anterior and scalenus middle muscles. Before passing over the first rib on its way out of the cervicoaxillary canal, the subclavian artery gives off branches, including the thyrocervical, internal mammary, and vertebral arteries. It becomes the axillary artery after it exits from behind the pectoralis minor muscle. Compression of this artery can lead to poststenotic dilation, stenosis, aneurysmal formation, or occlusion.

The subclavian vein travels from the arm and goes behind the pectoralis minor muscle before going between the first rib and clavicle. This space is bounded medially by the costoclavicular ligament and laterally by the scalenus anterior muscles as it inserts onto the first rib. Compression of the vein occurs in this area and can lead to stenosis and occlusion.

The brachial plexus is composed of nerve roots from the C5 through the T1 vertebral foramina. These nerve roots join to form the superior trunk (C5 and C6), the middle trunk (C7), and the inferior trunk (C8 and T1). These trunks separate into anterior and posterior divisions that fuse again to form lateral, medial, and posterior cords of the brachial plexus. The plexus travels through the tunnel formed by the anterior and middle scalene muscles. It travels between the first rib and the clavicle and finally under the pectoralis minor muscle to gain access to the arm.

In the normal anatomy, there is ample room for each of these structures. There are four major areas in which the vessels or nerves can be compressed (Table 1-1).This topic will be discussed in detail in Chapter 26.

Diaphragm

The diaphragm, at the inferior thoracic aperture, separates the thoracic cavity from the abdominal cavity. The inferior thoracic aperture, which slopes inferoposteriorly, is limited by the 12th thoracic vertebra posteriorly, the 12th pair of ribs and costal margins anterolaterally, and the xiphisternal joint anteriorly.

The diaphragm is a curved, musculotendinous sheet that is mainly convex toward the thoracic cavity. It is a continuous sheet of muscle with low posterior and lateral attachments and high anterior attachments. The central tendon is a thin but strong aponeurosis. The domes of the diaphragm descend 2 cm during quiet respiration and can travel as much as 10 cm during heightened respiratory requirements. During expiration, the right diaphragm can rise as high as the level of the nipple, whereas the left rises to a level one rib space lower. With maximal inspiration, the diaphragm flattens against the abdominal contents. The right diaphragm can flatten to the level of the 11th rib, whereas the left can flatten to the level of

TABLE 1-1 **Sites and Structures Compressed in Thoracic Outlet Syndrome**

Site	Description	Abnormalities	Structures Compressed
Sternal-costovertebral circle	This aperture can be narrowed by bony variations	Cervical first rib First rib Long transverse process	Subclavian artery Subclavian vein Brachial plexus
Scalene muscle triangle	The scalenus anterior and middle muscle insert on the first rib, creating a tunnel	Scalenus anterior and middle	Subclavian artery Brachial plexus
First rib, clavicular space	The neurovascular structures lie above the rib and below the clavicle	Costoclavicular ligament Clavicle First rib	Subclavian vein Subclavian artery Brachial plexus
Behind the pectoralis minor muscle	The neurovascular structures travel to and from the arm behind this muscle	Pectoralis minor Costocoracoid ligament	Subclavian vein Subclavian artery Brachial plexus

the 12th rib. The right diaphragm has to work against the liver, whereas the left needs to push only against the stomach and spleen; therefore, the right diaphragm has significantly stronger fibers than the left.

The costal diaphragm receives its blood supply from the lower five intercostal and subcostal arteries, and the central portion is supplied by the phrenic arteries. The phrenic arteries can arise directly from the aorta, above the celiac axis, as a common trunk or individually. Occasionally, they arise from the celiac or renal arteries. The sole motor supply to the diaphragm is the phrenic nerve. It also supplies sensory fibers to the parietal and peritoneal pleura overlying the diaphragm; this accounts for the diaphragmatic irritation that is sometimes interpreted as ipsilateral shoulder pain.

The diaphragm has several openings through which structures can transverse from one cavity to another (see Fig. 1-1*B*). The inferior vena cava hiatus lies anteriorly and to the right of the midline, at the level of vertebra T8. The right phrenic nerve travels through this hiatus, and the left phrenic nerve penetrates laterally through its own opening at the same level. The esophageal aperture is at the level of the T10 vertebra, and the right and left vagal trunks that adhere to it enter the abdomen along with the esophagus.

The aortic aperture, at the T12 vertebral level, is formed by the interdigitating fibers (median arcuate ligament) of the right and left diaphragmatic crura. The azygos and hemiazygos veins and the thoracic duct also pass through this opening.

The greater and lesser splanchnic nerves gain access to the abdominal cavity via two small apertures in each of the crura, and musculophrenic branches of the internal mammary artery penetrate the diaphragm through small apertures near its connection with the costal cartilages of ribs seven to nine.

Diaphragmatic hernias can develop through known openings, such as a hiatal hernia through the esophageal hiatus, or through congenital defects. The most common congenital abnormality is a Bochdalek hernia, in which abdominal contents go through a posterolateral defect. This abnormality is seen more commonly on the left side. A Morgagni hernia, however, occurs with a defect in the anterior aspect of the diaphragm just lateral to the xiphoid.

Bony Thoracic Cage

Sternum

The sternum or breastbone is made of cancellous bone and filled with hemopoietic marrow throughout life. The main parts, the manubrium and body, are connected by a secondary cartilaginous joint that normally never ossifies and contributes to movement of the ribs.

Up to puberty, the six segments, or sternebrae, are held together by hyaline cartilage. The central four segments fuse to form the body of the sternum between 14 and 21 years of age. The manubrium sterni (superiorly) and the xiphoid process (inferiorly) remain separate.

The manubrium receives the sternal ends of the clavicles in a shallow concave facet. The widest portion of the manubrium has bilateral costal incisurae that articulate with the first costal cartilage to form a primary cartilaginous joint. The second costal cartilage articulates with both the lower lateral ends of the manubrium and the body of the sternum, forming separate synovial joints. The muscular attachments of the manubrium include the sternocleidomastoid muscle, the sternohyoid and the sternothyroid superiorly, and the pectoralis major muscle anterolaterally. Most of the posterior surface is bare bone, which can be in contact with the brachiocephalic vein unless thymic remnants lie between.

The gladiolus, or body of the sternum, is slanted at a steeper angle than the manubrium; its articulation with that bone forms the sternal angle. Ossification of this joint, synchondrosis, in adult life can limit normal movement at this joint. The articular facets for ribs two to seven lie along the lateral border of the body of the sternum. These make single synovial joints with the costal cartilages. The facets for the sixth and seventh costal cartilages can coalesce, especially in females. The lateral border gives attachment to the anterior intercostal membrane and the internal intercostal muscles, and the pectoralis major arises anteriorly. Weak sternopericardial ligaments pass into the fibrous pericardium.

The cartilaginous xiphoid may be bifid or perforated, is of variable length, and usually ossifies in the fourth decade of life. The costoxiphoid ligaments prevent its displacement during diaphragmatic contractions.

Ribs

The 12 pairs of ribs are divided into the upper seven, which are called *true ribs* or *vertebrosternal ribs* because they form complete loops between the vertebrae and the sternum, and the lower five ribs, which fail to reach the sternum and are considered false ribs. The 8th, 9th, and 10th ribs are called vertebrocostal because each of their costal cartilages articulates with the adjacent rib cartilage. Ribs 11 and 12 are free-floating or vertebral ribs because their only articulation is with their vertebrae.

Ribs three to nine are classified as typical ribs and have a head, neck, and a shaft. The head has an upper and a lower articular facet divided by a crest for articulation with two adjacent vertebrae in synovial costovertebral joints, the lower facet articulating with the upper border of its own vertebra. The neck is flattened, with the upper border curling up into a prominent ridge—the crest. A tubercle projects posteriorly from the end of the neck and marks the junction of the neck and the body (Fig. 1-3).

MUSCLES OF THE THORAX

The muscles of the chest wall serve to protect the contents of the thoracic cavity, and they assist the movements of the thorax and upper extremities (Fig. 1-4). The 17 muscles of the chest wall are not discussed in detail here, but Table 1-2 lists them with their innervations and sites of attachments. This section focuses on muscle groups that are used in chest wall reconstruction. The latissimus dorsi, pectoralis major, serratus anterior, trapezius, rectus abdominis, and external oblique are the six major muscles that are available for reconstruction (Table 1-3).

The latissimus dorsi is the largest muscle of the thorax. It originates from the lower six thoracic spinous processes and from the lumbodorsal fiber, which is attached to the lumbar and sacral vertebrae. It also has fibers originating from the iliac crest. The muscle narrows and then inserts on the intertubercular groove of the humerus. It is supplied by the thoracodorsal artery, a branch of the subscapular artery. The subscapular artery arises from the axillary artery and gives a branch to the serratus anterior muscle before supplying the latissimus dorsi. The artery can be found on the undersurface of the latissimus dorsi. The mobile arterial supply and excellent musculocutaneous collaterals allow this muscle to be moved with or without its overlying skin.

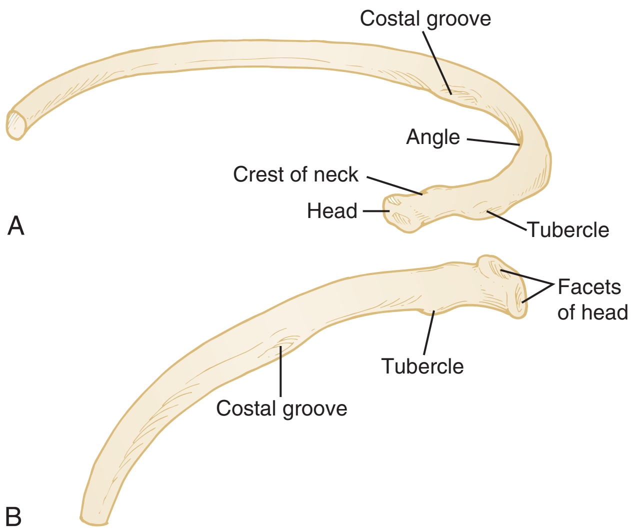

FIGURE 1-3 ■ Typical rib.

The pectoralis major muscle arises from the sternum, clavicle, and first seven ribs. It inserts on the bicipital humeral groove. It receives arterial supply from a pectoral branch of the thoracoacromial artery arising midclavicularly. It also receives some blood supply from the internal mammary, lateral intercostals, and lateral thoracic perforators. This flap is most frequently used for sternal defects.

Located between the latissimus dorsi and pectoralis major muscles is the serratus anterior muscle. This small muscle originates from the superior borders of the eighth through tenth ribs. It inserts on the tip of the scapula. Its blood supply is from a branch of the thoracodorsal artery and from the long thoracic artery. It can be used for intrathoracic purposes such as bronchial stump coverage or muscle interposition between the trachea and esophagus after a tracheoesophageal fistula repair.

The trapezius muscle arises from the occipital bone and from the spinous process of the seventh cervical vertebra and all the thoracic vertebrae. It inserts on the lateral aspect of the clavicle, the acromion process, and the spine of the scapula. It receives its blood supply from the transverse cervical artery. Although the trapezius is a large muscle, its use is limited to reconstruction of the upper thoracic cavity.

Arising from the inferior borders of the 4th through 12th ribs and inserting on the iliac crest is the external oblique muscle. It accepts blood supply from the lower thoracic intercostal arteries. Unlike the trapezius muscle, uses of the external oblique muscle are limited to the thoracic cavity below the inframammary crease.

The rectus abdominis muscle spans the entire anterior abdominal wall. It originates at the pubic crest and rises superiorly to insert on the fifth through seventh rib cartilages and xiphoid process. The superior and inferior epigastric arteries supply this vast muscle. It has been used for reconstruction of the anterior thoracic cavity, most notably after breast surgery.

Intercostal Muscles

Fibers of the intercostalis externi muscle arise from the sharp lower border of the rib above and course inferomedially (i.e., in the direction of the fingers when the hands are put into the front pockets of trousers) to the smooth upper border of the rib below. Anteriorly, it is replaced by the anterior intercostal membrane. Between the bony ribs is muscle; between the costal cartilages is membrane. In the lower spaces, the muscle interdigitates with the fibers of the external oblique (Fig. 1-5).

The intercostalis interni muscle runs from the lower costal groove of ribs 1 to 11, to the upper surfaces of ribs 2 to 12 downward and backward. Anteriorly, the muscle extends up to the sternum, but posteriorly only up to the

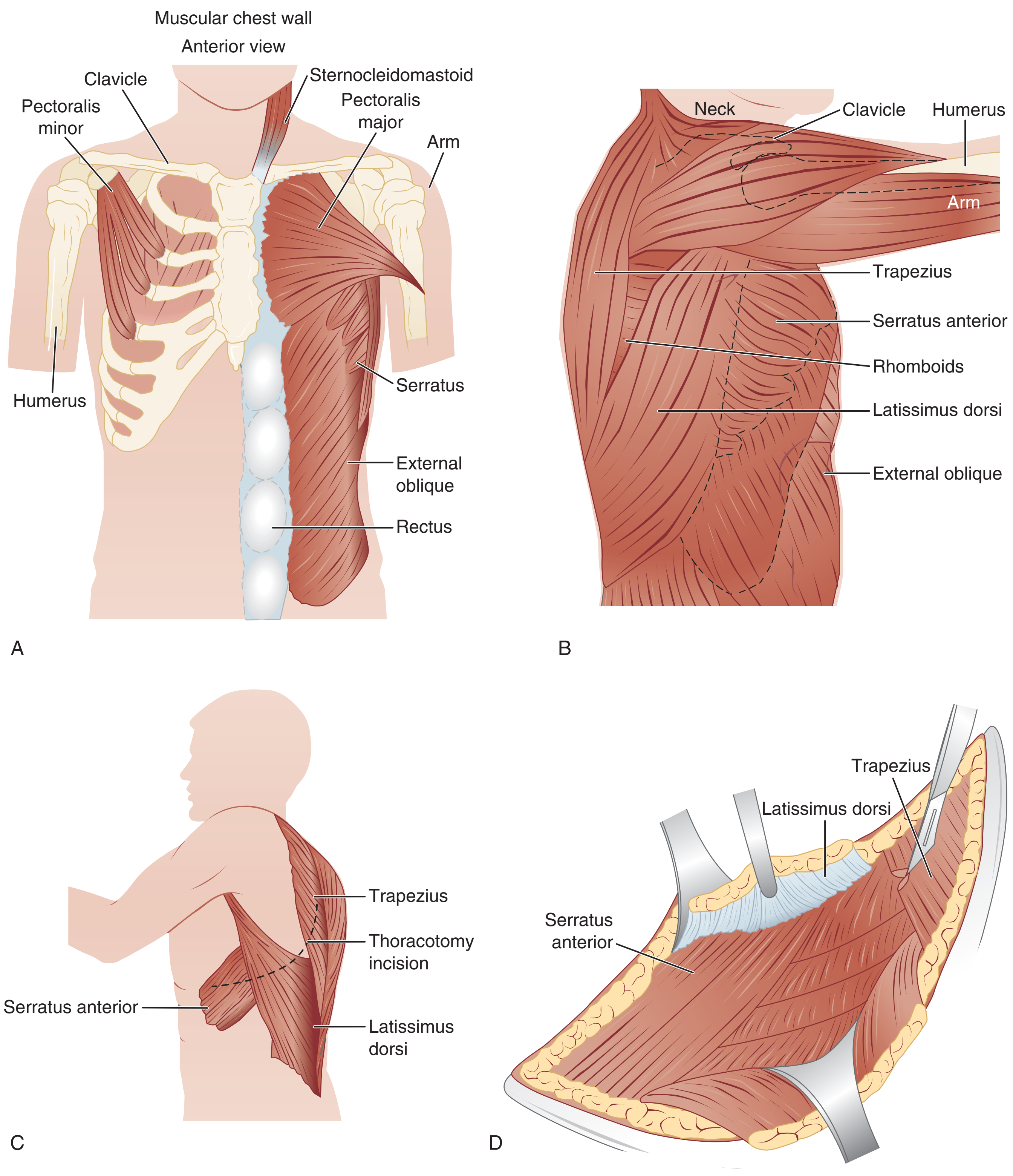

FIGURE 1-4 ■ **A,** Anterior view of major muscles of the chest wall. **B,** Lateral view of the muscles of right hemithorax. **C,** *Dotted line* indicates placement of a standard posterolateral thoracotomy. **D,** Incisional view of muscles encountered during a posterolateral thoracotomy.

TABLE 1-2 Attachments and Innervation of the Muscles of the Thoracic Wall

Muscle	Proximal Attachments	Distal Attachments	Innervation
Pectoralis major sternocostal head	Half of sternum, costal cartilages 1 to 6, aponeurosis of external obliquus muscle	Lateral lip of intertubercular sulcus of humerus	Medial pectoral nerve (C8-T1)
Pectoralis major clavicular head	Medial half of clavicle	Lateral lip of intertubercular sulcus of humerus	Lateral pectoral nerve (C5, 6, 7)
Pectoralis minor	Ribs 3 to 5	Coracoid process of scapula	Medial pectoral nerve
Subclavius	First rib	Medial clavicle	Nerve to subclavius (C5-6)
Deltoid	Lateral third of clavicle, acromion, and spine of scapula	Deltoid tuberosity of humerus	Axillary nerve (C5-6)
Serratus anterior	Angles of superior 10 ribs	Medial border of scapula	Long thoracic muscle nerve (C5, 6, 7)
Supraspinatus	Supraspinous fossa of the scapula, fascia of trapezius	Greater tubercle of the humerus	Suprascapular nerve (C5)
Infraspinatus	Infraspinous fossa	Greater tubercle of the humerus	Suprascapular nerve
Subscapularis	Costal surface of the scapula	Lesser tubercle of the humerus and its crest	Upper (C5-6) and lower (C5, 6, 7) subscapular nerve
Latissimus dorsi	Spinous processes of T7-12, L1-5, S1-3 vertebrae, posterior part of iliac crest, lower three to four ribs	Crest of the lesser tubercle and floor of the intertubercular groove of the humerus	Thoracodorsal nerve (C6-7)
Serratus posterior inferior	Spine of C6-T2 vertebrae	Angles of ribs 2 to 5	Segmental intercostal nerves
Serratus posterior superior	Spine of T11-L2 vertebrae	Lower border of ribs 9 to 12	Segmental intercostal nerves
Trapezius	Ligamentum nuchae, external occipital protuberance, thoracic vertebral spinous processes	Lateral one third of clavicle, acromion process along spine of scapula	Spinal accessory nerve
Levator scapulae	Transverse process of C1, C2, C3, C4 (cervical vertebrae)	Medial border of scapula, superior angle to base of scapular spine	Dorsal scapular nerve (C5)
Rhomboid major and minor	Spinous processes of C7-T5 and supraspinous ligaments	Medial border of scapula up to the inferior angle	Dorsal scapular nerve (C5)
Teres major	Lower lateral border of the scapula	Crest of the lesser tubercle of the humerus	Lower subscapular nerve (C5, 6, 7)
Teres minor	Mid to upper lateral border of the scapula	Greater tubercle of the humerus	Axillary nerve (C5-6)

TABLE 1-3 Arterial Supply of Muscles Used in Chest Wall Reconstruction

Muscle	Arterial Supply
Latissimus dorsi	Thoracodorsal artery
Pectoralis major	Thoracoacromial, lateral thoracic perforators, internal mammary artery, lateral intercostal artery
Serratus anterior	Thoracodorsal artery, long thoracic artery
Trapezius	Transverse cervical artery
External oblique	Lower thoracic intercostal arteries
Rectus abdominis	Superior and inferior epigastric arteries

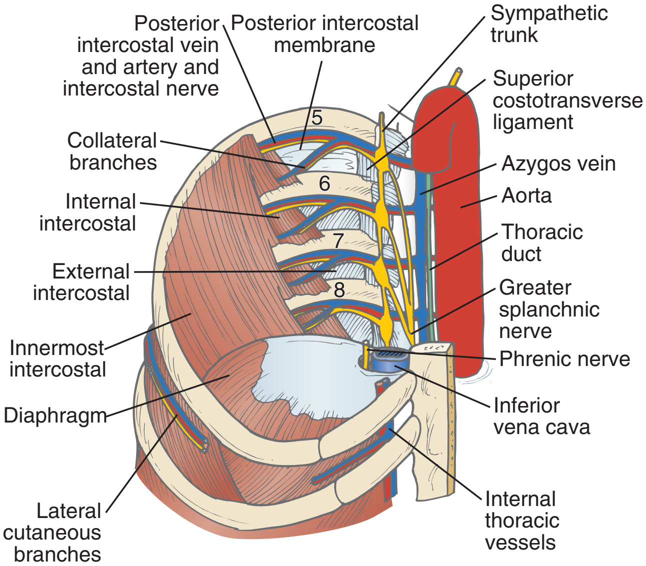

FIGURE 1-5 ■ Spatial organization of the thoracic wall on the right side.

angles of the rib. Beyond that, it is replaced by the internal intercostal membrane, which attaches to the tubercle of each rib and vertebra.

The innermost or transversus layer is divided into three groups: the innermost intercostals (anterolateral), subcostal (posterior), and transversus thoracis (anteromedial) muscles. The fibers run downward and backward, as in the internal intercostal muscles. The subcostal muscles lie in the paravertebral gutter, are better developed inferiorly, and cross more than one space. The transversus thoracis was formerly called the *sternocostalis*, a more appropriate name. Digitations arise from the sternum bilaterally to the costal cartilages of ribs two to six.

The intercostalis intimi muscles also traverse more than one space and are better developed in the lower lateral spaces. The neurovascular bundle runs in the plane between the innermost and outer two layers. From above downward, the order is vein, artery, and nerve (mnemonic: VAN). Beyond the angle of the rib posteriorly, they are protected by the downward projection of the lower border of the rib. For a thoracotomy, the periosteum is stripped off the upper half of the rib, avoiding the lower border and the neurovascular bundle (Fig. 1-6).

As in the rest of the body, the mixed spinal nerve is formed from a dorsal and a ventral root, the dorsal root being sensory and the ventral root containing somatic motor neurons. As it emerges from the intervertebral foramina, it branches into a dorsal and a ventral ramus. The dorsal ramus of the thoracic spinal nerve supplies the paravertebral back muscles and skin of the back. The ventral ramus communicates with the sympathetic chains via white rami communicantes (postganglionic fibers). Beyond this point, the true intercostal nerve lies just superficial to the parietal pleura in the endothoracic fascia. It gains the costal groove between the innermost intercostal and the internal intercostal muscles near the angle of the rib, where a collateral branch is given off. This small branch supplies the muscles of the space, the

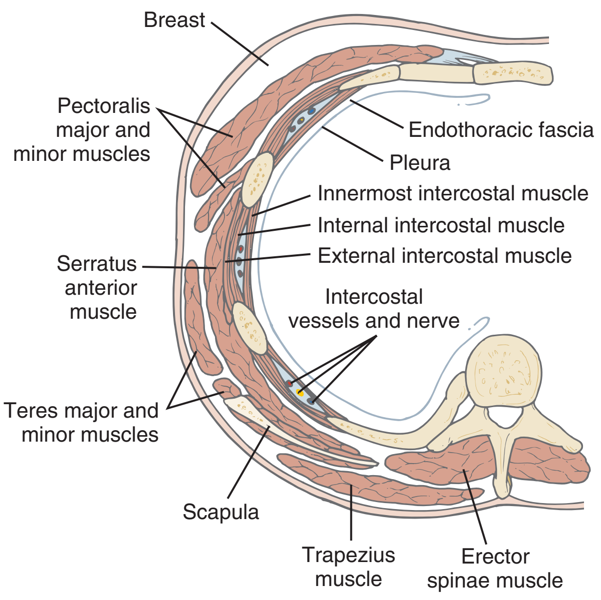

FIGURE 1-6 ■ Layers of the chest wall.

parietal pleura, and the periosteum of the rib. The main nerve itself has muscular branches, a lateral cutaneous branch, and a terminal anterior cutaneous branch. The lateral cutaneous branch given off along the midaxillary line gives off anterior and posterior branches to supply the skin over that space. Just lateral to the sternal margin, the terminal anterior cutaneous branches of the upper six nerves pierce the internal intercostal muscles, the external intercostal membrane, and the pectoralis major to reach skin. The lower five intercostal nerves slope downward behind the costal margin into the neurovascular plane of the abdominal wall. The subcostal or 12th thoracic nerve leaves the thorax by passing behind the lateral arcuate ligament and the subcostal artery and vein (Fig. 1-7). The cutaneous branches of each dermatome tend to overlap considerably; hence anesthesia after thoracic incisions is quite rare unless multiple intercostal nerves have been damaged. The first intercostal nerve is very small and supplies no skin, lacking both lateral and anterior cutaneous branches.

Two sets of intercostal arteries, the posterior and the anterior, are responsible for supplying the intercostal spaces. Their course and branching patterns closely conform to those of the intercostal nerves. The posterior intercostal arteries are branches of the descending thoracic aorta except in the first two spaces, where they are branches of the supreme intercostal artery, given off by the costocervical trunk of the second part of the subclavian artery. The aortic branches lie on the left side of the mediastinum; consequently, the right posterior intercostal arteries are longer, can be easily dissected in the left chest, and are seen best while operating on descending thoracic aortic aneurysms.

The anterior intercostal arteries are branches of the internal thoracic arteries from the first part of the subclavian artery. The internal thoracic artery runs anterior to the transversus thoracis and on the internal surface of the costal cartilages and the internal intercostal muscles. Approximately one fingerbreadth from the border of the sternum running vertically downward, the artery gives off two anterior intercostal arteries in each space. At the costal margin, below the sixth costal cartilage, the artery divides into the superior epigastric and musculophrenic arteries. The anterior intercostal arteries are smaller than the posterior intercostal arteries with which they anastomose and run predominantly along the lower border of each costal cartilage in the same fascial neurovascular plane. In the lower spaces, they are branches of the musculophrenic artery. There are no true anterior intercostal arteries in the last two spaces.

The internal thoracic arteries also give branches to the mediastinum, the thymus, the pericardium, and the sternum, and especially large perforating branches in the second to fourth space, the predominant supply to the lactating breast in females.

In each space, there are one posterior and two anterior intercostal veins, designated by names identical to the arteries that they accompany. The veins lie above the artery and the nerve throughout their course (i.e., VAN) in the intercostal space. The anterior veins drain into the musculophrenic and internal thoracic veins. The vein of the first space or the supreme intercostal vein, posteriorly,

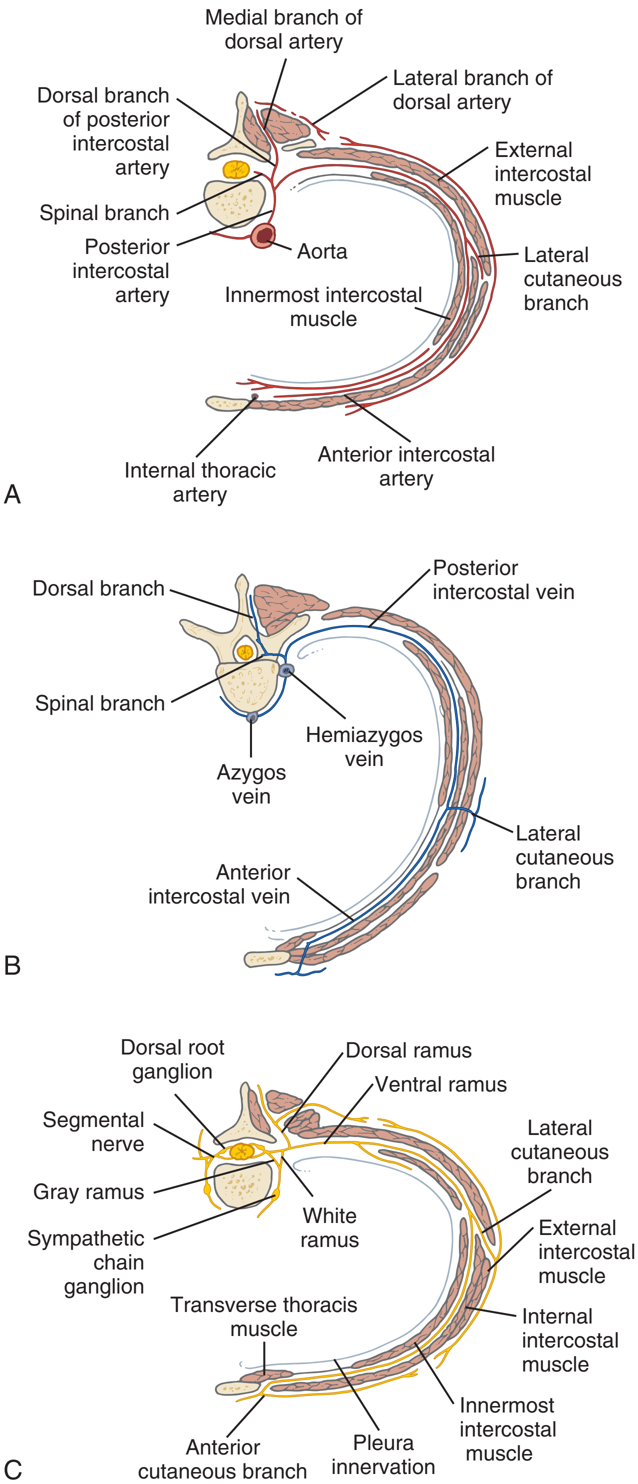

FIGURE 1-7 ■ Organization of the intercostal space and the relationship of the arteries **(A)**, veins **(B)**, and nerves **(C)** to the muscle layers.

may be a tributary of the brachiocephalic, vertebral, or superior intercostal vein. The superior intercostal vein is formed by the posterior intercostal veins of the second, third, and sometimes the fourth spaces. This vein drains into the azygos vein on the right side, and on the left side it arches over the aorta, superficial to the vagus and deep to the phrenic to open into the left brachiocephalic veins. Subcostal veins join the ascending lumbar veins and ascend on the left side as the hemiazygos and on the right side as the azygos vein draining the lower eight spaces. The blood in the hemiazygos vein drains across the midline, through median anastomoses into the azygos vein.

The internal thoracic vessels are part of the anastomotic chain that links the subclavian artery and brachiocephalic veins to the external iliac vessels. The intercostal vessels in turn connect to the descending aorta and azygos system of veins. In the presence of obstruction to flow, these anastomoses provide alternative channels for arterial and venous blood flow.

Anatomy of Breathing

Simple respiratory effort is attained mostly by diaphragmatic motion. The bony and muscular components of the thorax remain a stable cavity while the diaphragm acts as a piston. It flattens during inspiration to create negative intrathoracic pressure, resulting in expansion of the lungs. Once inspiration is complete, the diaphragm relaxes and the lung recoils to its original position. The intercostal muscles are important to prevent paradoxical motion during inspiration.

The thoracic cavity can change to meet increased respiratory needs. The accessory muscles of the chest wall help to increase intrathoracic volume during inspiration and decrease volume during expiration. In addition to the piston action of the diaphragm, the accessory muscles elevate the sternal body and xiphoid process anteriorly and superiorly. The lower ribs attached to the sternum follow this movement and therefore increase the diameter of the lower chest cavity. The manubrium of the sternum is relatively fixed, and the chest cavity at this level does not contribute significantly to increased respiratory needs. This dynamic response of the chest cavity helps to meet increasing demands for oxygenation and ventilation.

SURFACE ANATOMY

An understanding of surface anatomy enables identification of bony and prominent structures and hence the position of deeply related structures (Fig. 1-8 and Table 1-4). The chest radiograph (Fig. 1-9) is an extension of the routine physical examination.

The suprasternal notch on the superior aspect of the manubrium is palpable between the prominent medial ends of the clavicle, and it lies at the level of the lower border of the body of the second thoracic vertebra. At the lower sternal border, the palpable xiphisternum is covered by the rectus abdominis muscles. The xiphisternal joint lies opposite the body of the ninth thoracic vertebra. The sternal angle of Louis (the junction of the manubrium with the body of the sternum) is an important landmark for the description of structures inside the chest. At this level, the second costal cartilage joins the lateral margin of the sternum. The sternal angle lies opposite the lower border of the fourth thoracic vertebral

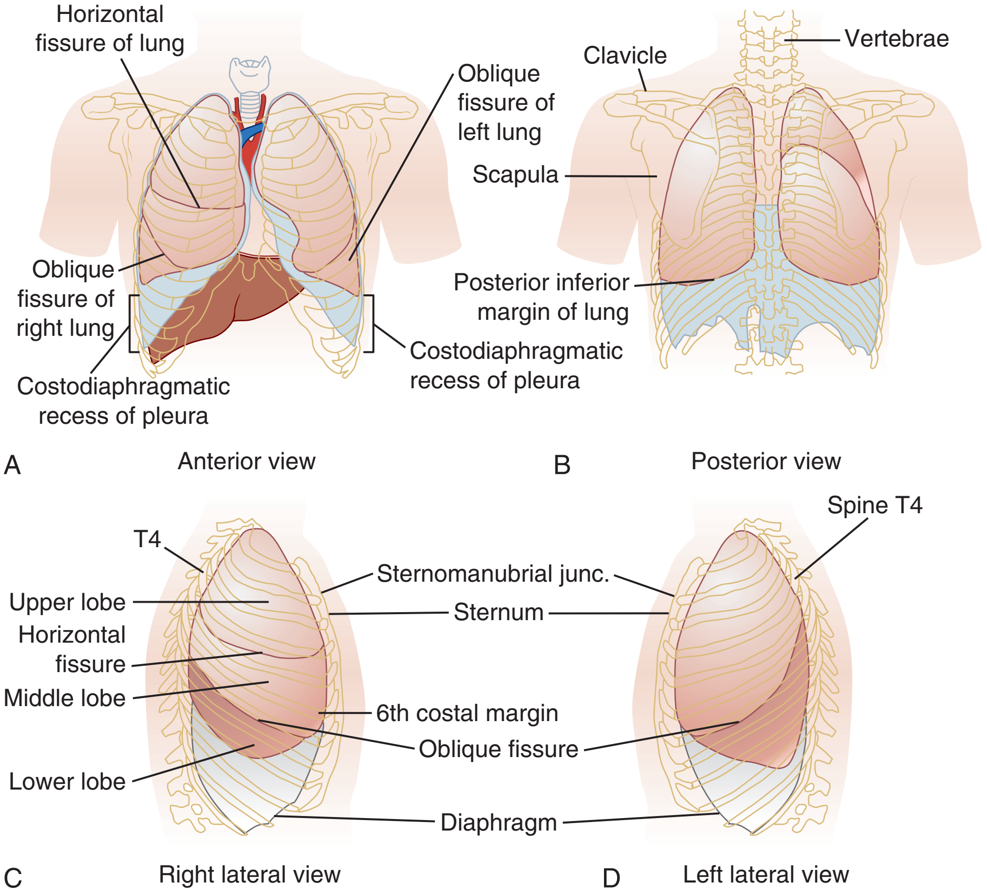

FIGURE 1-8 ■ Correlation of lungs and overlying bony structures. **A,** Anterior view. **B,** Posterior view. **C,** Right lateral view. **D,** Left lateral view. The right oblique fissure courses anteriorly at the level of the fifth rib, ending near the level of the sixth rib. The posteriorly left oblique fissure is more variable, starting at a level between the third and fifth ribs. Anteriorly, it ends consistently at the level of the fifth rib. The horizontal fissure starts anteriorly at the fourth costal cartilage and joins the oblique fissure at the level of the fifth rib.

TABLE 1-4 **Surface Landmarks and Correlating Intrathoracic Structures**

Landmark	Underlying Structures
Sternocleidomastoid muscle (SCM)	Internal jugular vein, cupola of pleura Internal mammary artery originates between sternal and clavicular heads of the SCM and runs 2 cm from sternal edge until the sixth costal cartilage
Right manubrial border	Right brachiocephalic vein, origin of superior vena cava, brachiocephalic artery
Manubrium	Aortic arch and origin of great vessels, left brachiocephalic vein
Left manubrial border	Left common carotid and left subclavian vessels
Angle of Louis	Trachea bifurcation Level of the fourth vertebral body
Body of sternum and third to sixth costal cartilages	Heart
At the level of the angle of Louis in the right hemithorax	Azygos vein joins superior vena cava Thoracic duct crosses midline
At the level of the angle of Louis in the left hemithorax	Aortic pulmonary window
Left third costal cartilage	Origin of aorta and pulmonary artery
Right third costal cartilage	Superior vena cava empties into right atrium
Sixth costal cartilage	Level of the eighth vertebral body Inferior vena cava and right phrenic nerve pass through the diaphragm
Left seventh costal cartilage	Tenth vertebral body Esophagus and vagal trunks pass through the diaphragm
Tip of the scapula	Seventh intercostal space

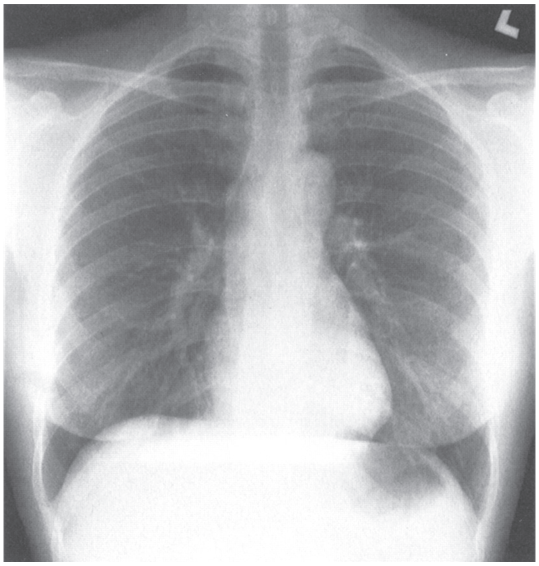
A

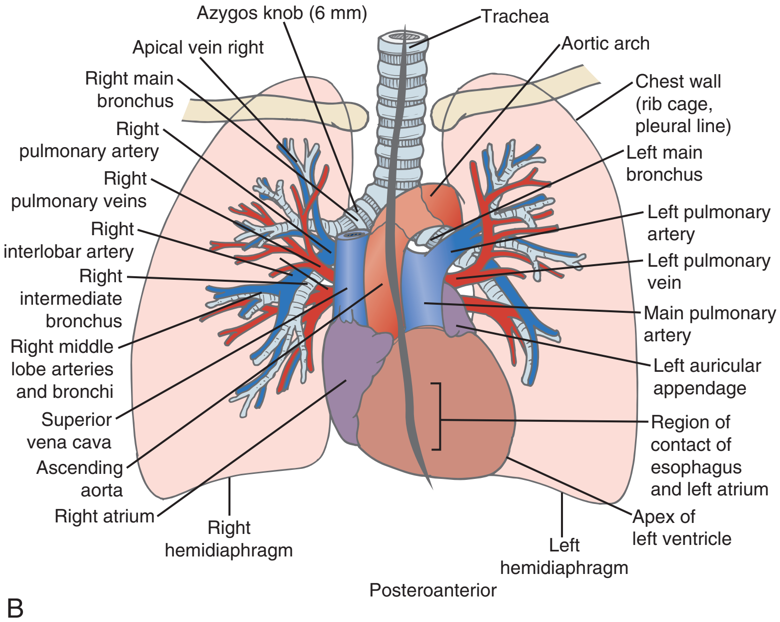

B

FIGURE 1-9 ■ **A,** Posteroanterior radiograph of the chest in a normal male adult. **B,** Schematic representation of the surface projection of intrathoracic structures seen on a normal chest radiograph. (From Butler P, Mitchell AWM, Ellis H: *Applied radiological anatomy.* Cambridge, 1999, Cambridge University Press.)

body. All other ribs are counted from this point, as the first rib is not palpable. The angle of Louis is a useful reference point for counting ribs on a computed tomography scan, and for localizing structures in the thoracic cavity. For example, the sternomanubrial joint is an important level for many structures. At this level, the azygous crosses midline to join the superior vena cava, the thoracic duct crosses from the right hemithorax to the left hemithorax on its ascent to the left neck, the trachea bifurcates into right and left main-stem bronchus, and the aorta and pulmonary artery form the aortic pulmonary window.

The clavicle articulates with the acromion process of the scapula laterally and the sternum medially. Just below the medial joint lies the fusion of the first ribs with the lateral margin of the sternum. The costal margin is the lower boundary of the bony thorax and is formed by the cartilages of the 7th, 8th, 9th, and 10th ribs and the ends of the 11th and 12th cartilages. The lowest part of the margin is the 10th rib, and it lies at the level of the third lumbar vertebra. The lower border of the pectoralis major muscle forms the anterior axillary fold. The tendon of the latissimus dorsi forms the posterior axillary fold as it passes around the lower border of the teres major muscle.

Posteriorly, the thoracic cage is covered by muscles (trapezius, latissimus dorsi, and erector spinae) and is obscured by the scapula, but there are a few useful landmarks to the rib levels. The superior angle of the scapula lies opposite the spine of the second thoracic vertebra. The transversely running spine of the scapula is easily felt and lies at the level of the third thoracic vertebra. The lower angle of the scapula overlies the seventh rib.

The first prominent spinous process in the low midline of the neck posteriorly is that of the seventh cervical vertebra, the vertebra prominens. The tip of a spinous process of a thoracic vertebra lies posterior to the body of the next vertebra below.

The apex of the pleura extends approximately 3 cm above the medial third of the clavicle and behind the sternocleidomastoid muscle. It passes downward and medially behind the sternoclavicular joints. The left pleura, at the level of the fourth costal cartilage, deviates laterally for a variable distance from the cardiac notch. Both pleurae lie at the level of the 8th rib in the midclavicular line, at the level of the 10th rib in the midaxillary line, and at the level of the 12th rib at the paravertebral level posteriorly.

The more constant right oblique fissure of the lung follows the course of the fifth rib from the midline posteriorly, more toward its lower border. Anteriorly it ends at the costochondral junction at the level of the sixth rib. The left oblique fissure has a more variable origin from the third to the fifth rib level, but anteriorly it follows a more predictable course along the fifth rib.

The transverse or horizontal fissure (present only on the right side) is marked by a horizontal line that runs backward from the fourth costal cartilage to reach the oblique fissure at the midaxillary line at the level of the fifth rib.

The pulmonary hilum lies laterally to the sternum behind the second to fourth costal cartilages and in front of the fourth to sixth vertebral bodies. The pulmonary trunk starts behind the left costal cartilage, and it ascends to the level of the second costal cartilage before it bifurcates. The aorta also arises from the heart at the level of the left third costal cartilage. It travels superiorly to the right side of the angle of Louis before arching leftward.

The great vessels arise from the aortic arch behind the sternomanubrial joint. The brachiocephalic artery travels under the manubrium toward the right sternoclavicular joint. The left common carotid artery makes a similar ascent under the manubrium but travels toward the left sternomanubrial joint before entering the neck. The left subclavian artery travels just left of the common carotid artery. The use of surface anatomy to guide incisions and approaches for various thoracic and cardiac procedures will be discussed in later chapters.

Transcribing a chest radiograph and a computed tomographic scan to a physical location on a patient is vital for any thoracic surgical procedure, but it is particularly important for video-assisted thoracic surgery (VATS). Often, small nodules are hard to palpate thoracoscopically unless a more localized area is identified. Anatomic landmarks can help to divide and further subdivide the lung to help localize these nodules (Fig. 1-10).

MEDIASTINUM

The mediastinum is centrally located in the thoracic cavity. A pleural cavity bounds each side of the mediastinum, and its inferior and superior borders are defined by the diaphragm and the thoracic inlet, respectively. In classic descriptions, the mediastinum is divided into a superior and inferior mediastinum. The superior mediastinum lies above the plane from the sternomanubrial joint to the fourth thoracic vertebra. In the superior compartment lies the upper part of the thymus, the lower ends of the strap muscles, and the upper half of the superior vena cava, trachea, thoracic duct, and esophagus. The inferior compartment is further subdivided into anterior, middle, and posterior.

In 2000, Shields recategorized the mediastinum into three compartments: anterior, middle, and posterior. The diaphragm and bilateral pleural cavities remain the inferior and lateral borders for each of these compartments. The superior border now extends to the thoracic inlet for each compartment. The anterior compartment lies between the sternum and pericardium and the great vessels. The posterior compartment lies behind the pericardium, great vessels, and tracheal bifurcation and extends to the vertebral column. The middle mediastinum is between the anterior and posterior compartments and includes the entire thoracic inlet (Table 1-5). Disease entities of the mediastinum are discussed in later chapters.

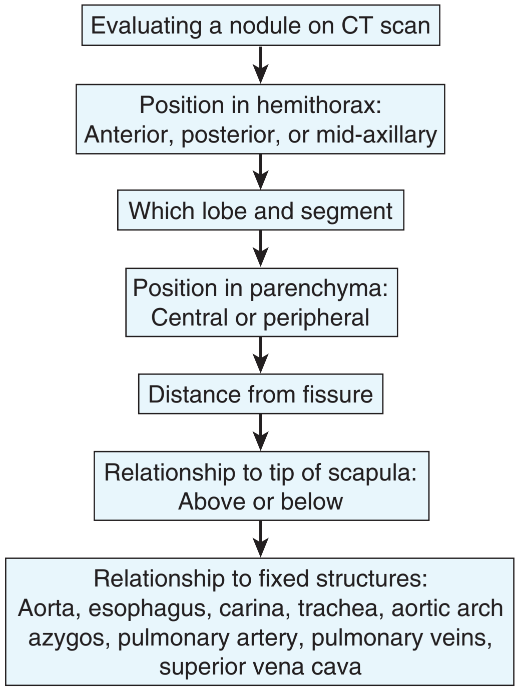

FIGURE 1-10 ■ Algorithm for correlating a pulmonary nodule on a computed tomographic (CT) scan for the patient during the operation.

TABLE 1-5 **Structures in the Mediastinum**

Compartment	Structures or Tissues	Pathologic Entities
Anterior	Thymus	Thymic disease
	Internal mammary artery	Teratoma
	Fat	Substernal thyroid
	Internal thoracic and prevascular lymph nodes	Disease of lymph nodes
	Connective tissue	Parathyroid disease
	Ectopic parathyroid	Bronchogenic cysts
	Substernal thyroid	
Middle	Heart	Lymph node disease (malignant and benign)
	Great vessels	Esophageal disease
	Trachea	Tracheal disease
	Proximal bronchi	Bronchogenic, pericardial, and esophageal cysts
	Vagus and phrenic nerves	Morgagni hernia
	Esophagus	Angiomas
	Thoracic duct	
	Proximal azygos vein	
	Descending aorta	
	Paratracheal lymph nodes	
Posterior	Sympathetic chain	Neurogenic tumors
	Distal azygos vein	Spinal lesions
	Posterior paraesophageal lymph nodes	

TRACHEOBRONCHIAL TREE

The trachea is a continuation of the larynx at the infracricoid level. Its average length is 11.8 cm. It has approximately 17 to 21 incomplete cartilaginous rings (4 mm wide and 1 mm thick) that maintain its elliptical shape in adults, but the shape is more circular in children. The coronal dimensions in men and women are 13 to 25 mm and 10 to 21 mm, respectively. The sagittal dimensions also differ between the sexes: 13 to 27 mm in men and 10 to 23 mm in women. With flexion of the neck, the trachea becomes almost completely an intrathoracic organ, coursing backward and downward from a subcutaneous position to rest ultimately on the esophagus and vertebral column at the level of the carina. Bearing a common embryologic origin with the esophagus, these two structures remain in intimate contact with one another, with the posterior muscular membranous wall of the trachea resting on the esophagus. The thyroid is anterior to the trachea in the neck and in the mediastinum, the thymus and parts of some of the great vessels lay anterior to the distal trachea.

The isthmus of the thyroid crosses the trachea at the second ring. The innominate artery crosses the mid trachea obliquely from right to left, and the arch of the aorta indents the esophagus slightly and appears to shift the trachea toward the right, away from its midline position. Lateral structures on the right side are predominantly venous and include the superior vena cava, azygos, and right brachiocephalic veins; lateral arterial structures on the left side include the arch of the aorta and the left common carotid artery. Both right and left vagi, along with their recurrent laryngeal nerves and the right and left sympathetic trunks, are also laterally related to the trachea. These intimate relationships of the trachea with surrounding organs are of important concern when performing cervical mediastinoscopy with lymph node biopsy.

Segmental blood supply to the trachea is from the inferior thyroid, subclavian, supreme intercostals, internal thoracic, innominate, and superior and middle bronchial arteries. This blood supply is shared with the esophagus and the main bronchi. Anastomotic arcades develop on the lateral tracheal wall and feed transverse vessels that travel between cartilaginous rings. For this reason, the trachea should not be devascularized circumferentially for a distance greater than 1 to 2 cm. The lateral arcades allow safe pretracheal dissections. Lymph drains to the posterior inferior group of deep cervical nodes and to paratracheal nodes.

The trachea bifurcates into the right and left principal bronchi (Fig. 1-11). The right principal bronchus arises in a more direct line with the trachea at an angle of approximately 25 degrees and passes behind the superior vena cava to reach the hilum of the lung. The left principal bronchus is slightly smaller, leaves the trachea more obliquely at an angle of approximately 45 degrees, passes below the arch of the aorta and the left pulmonary artery, and is almost twice as long as the right main bronchus

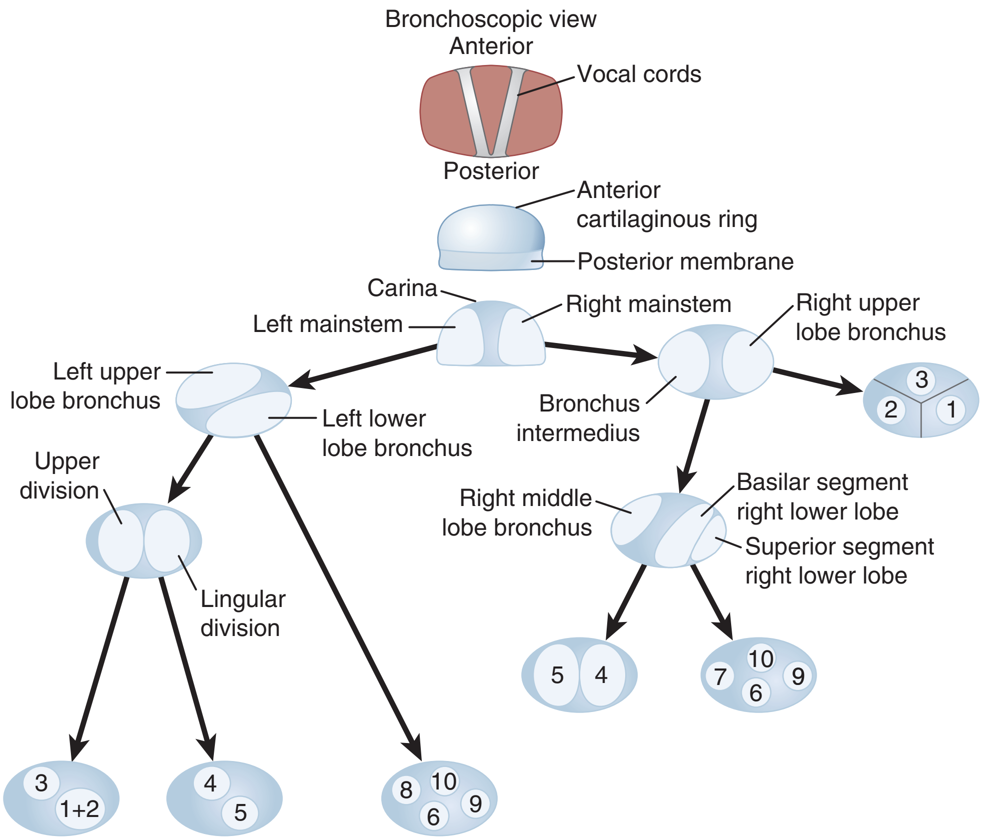

FIGURE 1-11 ■ Bronchoscopic view of the tracheobronchial tree. See Figure 1-12 for names of the numbered segments.

(4 to 6 cm). The carinal angle can be wider in women and obese people. It can also be wider in patients with bulky subcarinal nodal disease.

The right upper lobe bronchus, also known as the *eparterial bronchus*, branches from the lateral wall of the right principal bronchus approximately 1.2 cm distal to the trachea. The upper lobe bronchus, approximately 1 cm in length, gives off three segmental bronchi as it makes almost a 90-degree angle with the right main bronchus and the bronchus intermedius. After a distance of approximately 1.5 to 2 cm, the middle lobe bronchus arises from the anterior surface of the bronchus intermedius. The middle lobe bronchus is 1.5 to 2.2 cm long and bifurcates into lateral and medial branches. The superior segmental bronchus to the lower lobe arises from the posterior wall of the bronchus intermedius as it terminates into the basal-stem bronchus that sends off segmental bronchi to the medial, anterior, lateral, and posterior basal segments. The medial basal segment arises anteromedially, whereas the lateral basal and posterior basal segments most often arise as a common stem.

The longer left principal bronchus bifurcates into the upper lobe bronchus that travels anterolaterally and the lower lobe bronchus that continues posteromedially. The left upper lobe bronchus divides into the superior and inferior divisions that supply the upper lobe and lingula, respectively. The superior division branches into an apical posterior segmental bronchus and an anterior segmental bronchus. The inferior or lingual bronchus, which is the equivalent of a middle lobe bronchus on the right, is 1 to 2 cm long and divides into the superior and inferior divisions. The lower lobe bronchus on the right side gives off the superior segmental bronchus as its first branch before the basal trunk continues for about 1.5 cm as a single trunk; this then bifurcates into an anteromedial basal segmental bronchus and a common bronchial stem for the remaining basal segments.

Anatomic variations usually involve segmental bronchi arising as a common stem. Occasionally, additional bronchi arise from the main stem and distribute to a segment that has its own bronchus. A right upper lobe bronchus originating from the trachea (a porcine tracheobronchial tree) occurs in 3% of the population. Recognizing aberrant tracheobronchial anatomy is important for placement of the double-lumen endotracheal tube and for performing the ensuing surgical procedure.

LUNGS

To conserve healthy tissue and to perform operations safely on the lung, the thoracic surgeon must have a thorough knowledge of the segmental bronchopulmonary anatomy. Developing as outpouchings of the foregut, the ventral lung buds undergo repeated branching to yield approximately 20 generations from the principal bronchi to the terminal alveolar sacs. With the bronchus at the center, each bronchopulmonary segment functions as an individual unit with its own pulmonary arterial and venous supply. Importantly, the pulmonary veins run in the intersegmental plane and do not accompany the bronchus and the pulmonary artery to each unit.

The lungs are free of the pleural cavity except for attachments to the heart, trachea, and inferior pulmonary ligaments. The larger right lung has three lobes—upper, middle, and lower—and is composed of 10 bronchopulmonary segments. The left lung has two lobes—upper and lower—and eight segments (Fig. 1-12). The lingula on the left side is the anatomic equivalent of the middle lobe and is incorporated into the upper lobe. The terminology proposed by Jackson and Huber for the pulmonary segments and the branches supplying them has been universally adopted. The apparent discrepancy of there being only eight segments on the left side is explained by the fact that the apical and posterior segmental bronchi of the left upper lobe and the anterior and medial segmental bronchi of the left lower lobe originate from a common stem bronchus (Fig. 1-13 and Table 1-6).

The oblique fissure on each side separates the lower lobe from the rest of the lung. Anomalous fissures of varying depth may be seen along any of the segments, but they are most commonly seen separating the superior

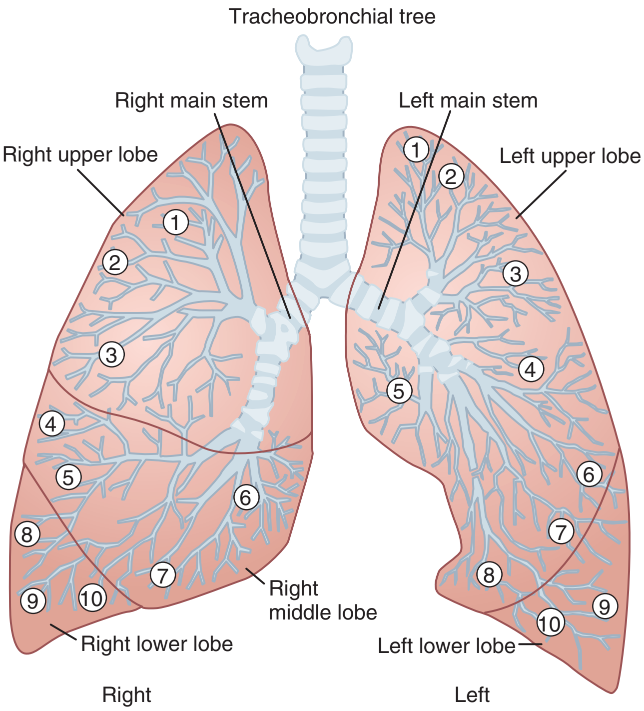

RUL
1. Apical segment
2. Posterior segment
3. Anterior segment

RML
4. Lateral segment
5. Medial segment

RLL
6. Superior segment
7. Medial basal segment
8. Anterior basal segment
9. Lateral basal segment
10. Posterior basal segment

1. & 2. Apical posterior segment
3. Anterior segment
4. Lingular superior segment
5. Lingular inferior segment
6. Basal superior segment
7. Lateral basal segment
8. Anterior medial basal segment
9. Lateral basal segment
10. Posterior basal segment

FIGURE 1-12 ■ Segments of the right and left lung. *RLL,* Right lower lobe; *RML,* right middle lobe; *RUL,* right upper lobe.

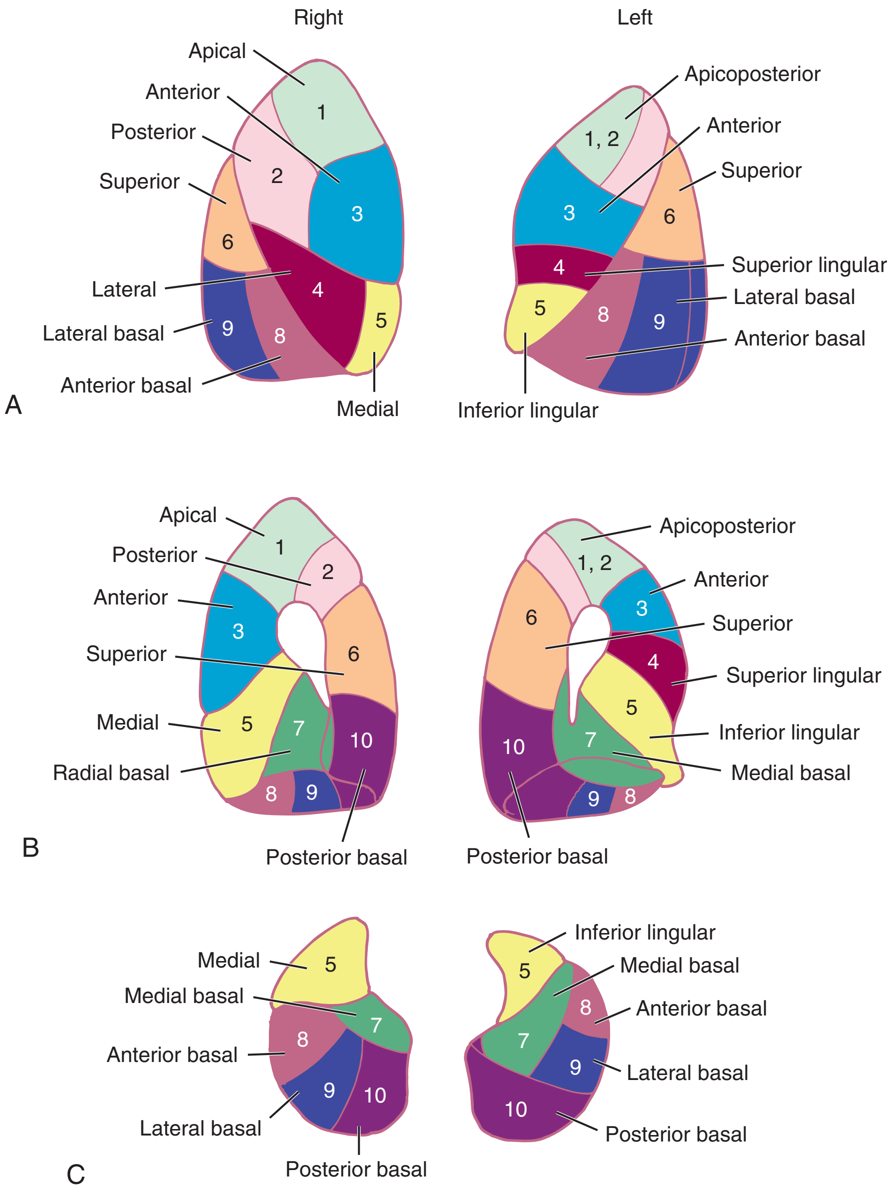

FIGURE 1-13 Bronchopulmonary segments. **A,** Lateral surface. **B,** Medial surface. **C,** Diaphragmatic surface.

TABLE 1-6 **Pulmonary Segmental Classification**

Right	Left
Upper Lobe	**Upper Lobe**
1. Apical	1. Apical posterior
2. Posterior	2. Apical posterior
3. Anterior	3. Anterior
Middle Lobe	**Lingula**
4. Lateral	4. Superior lingula
5. Medial	5. Inferior lingula
Lower Lobe	**Lower Lobe**
6. Superior	6. Superior
7. Medial basal	7. Anteromedial basal
8. Anterior basal	8. Anteromedial basal
9. Lateral basal	9. Lateral basal
10. Posterior basal	10. Posterior basal

segment of the lower lobe. Rarely, the apical segment of the right upper lobe may be a true tracheal lobe, with its bronchus arising directly from the trachea. The azygos lobe is not a true segment, but is formed by the azygos vein cutting into the pleura and apex of the lung. Medlar evaluated 1200 lungs and found an incidence of incomplete oblique fissure on the left and right of 18% and 30%, respectively. Of these patients, 63% had an incomplete horizontal fissure.

The right and left hila have different characteristics (Table 1-7). The right hilum exits the mediastinum below the confluence of the azygos and superior vena cava, and behind the superior vena cava and right atrial juncture. The left hilum lies below the aortic arch. The position of the pulmonary artery is somewhat different on the two sides. On the left (Fig. 1-14), the artery lies anterior and superior to the bronchus and runs in a slightly posterior

TABLE 1-7 **Characteristics of Left and Right Lung and Their Lobes**

Side or Lobe	Characteristics
Right lung	Hilum enters behind the superior vena cava or the right atrial juncture below the azygos nerve Ten segments Three lobes with a horizontal and oblique fissure The most superior and posterior structure in the right hilum is the right main-stem bronchus The right pulmonary artery is superior and slightly posterior to the right superior pulmonary vein The right pulmonary artery is inferior and anterior to the right main-stem bronchus Pulmonary veins most often enter heart separately
Left lung	Hilum courses under aortic arch Eight segments Two lobes with an oblique fissure Left pulmonary artery lies anterior and superior to the left main-stem bronchus The left superior vein is anterior and inferior to the left pulmonary artery Greatest variation in number and location of pulmonary artery branches Superior and inferior veins form common trunk before entering left atrium in 25% of the population
Right upper lobe	Arterial supply from truncus anterior branch coming off right main pulmonary artery at apex of hilum and from posterior ascending artery, found posterior to superior pulmonary vein or in fissure as ongoing pulmonary artery exits lung parenchyma Venous drainage into upper division of superior pulmonary vein Right upper lobe bronchus posterior in hilum Three segments
Right middle lobe	Arterial supply from one (45%) or two (48%) middle lobe arteries found from the right pulmonary artery at the confluences of the horizontal and oblique fissures Middle lobe vein drains most often into superior pulmonary vein and occasionally into inferior pulmonary vein Middle lobe bronchus from bronchus intermedius Two segments From anterior to posterior: middle lobe vein, bronchus, artery
Right lower lobe	Superior segmental artery and basilar artery are terminal branches of right pulmonary artery in the fissure Inferior pulmonary vein Right lower lobe bronchus Five segments From anterior to posterior: inferior pulmonary vein, pulmonary artery, bronchus
Left upper lobe	Two to eight arterial branches First branch of the pulmonary artery comes off behind superior pulmonary vein Varying number of posterior ascending arteries are given off after first branch as the pulmonary artery courses over and behind the left main-stem bronchus Lingular artery: most anterior branch in fissure going to upper lobe Superior pulmonary vein with upper division and lingular veins Four segments Left upper lobe bronchus posterior to vein
Left lower lobe	Superior segmental artery and basilar artery are terminal branches of right pulmonary artery in the fissure Inferior pulmonary vein Left lower lobe bronchus Four segments From anterior to posterior: inferior pulmonary vein, pulmonary artery, bronchus
Segments	Triangular parenchyma with apex toward center Bronchus runs in middle of segment Segmental artery on posterior surface of bronchus Veins in intersegmental planes Veins vary more than arteries, which vary more than bronchus Lingular and superior segmentectomies are easiest Basilar and apical segmentectomies harder Anterior segmentectomy hardest

direction before curving around and behind the left upper lobe bronchus. The right main-stem bronchus is the most superior and posterior of the right hilar structures, and the artery, though slightly anterior, is inferior to the bronchus (Fig. 1-15). The superior pulmonary veins are inferior and anterior to the pulmonary arteries, and the inferior pulmonary veins are even more inferior and posterior to the superior veins.

The main pulmonary artery arises to the left of the aorta and passes superiorly and to the left, anterior to the left main-stem bronchus, where it divides into the right and left main pulmonary arteries. The right pulmonary artery passes to the right behind the ascending aorta and forms the superior border of the transverse sinus. It then passes posterior to the superior vena cava and forms the superior border of the postcaval recess of Allison, whereas the right superior pulmonary vein forms the inferior border of the recess. The first branch is the truncus anterior (rarely intrapericardial); it arises superolaterally and supplies the upper lobe before the pulmonary artery

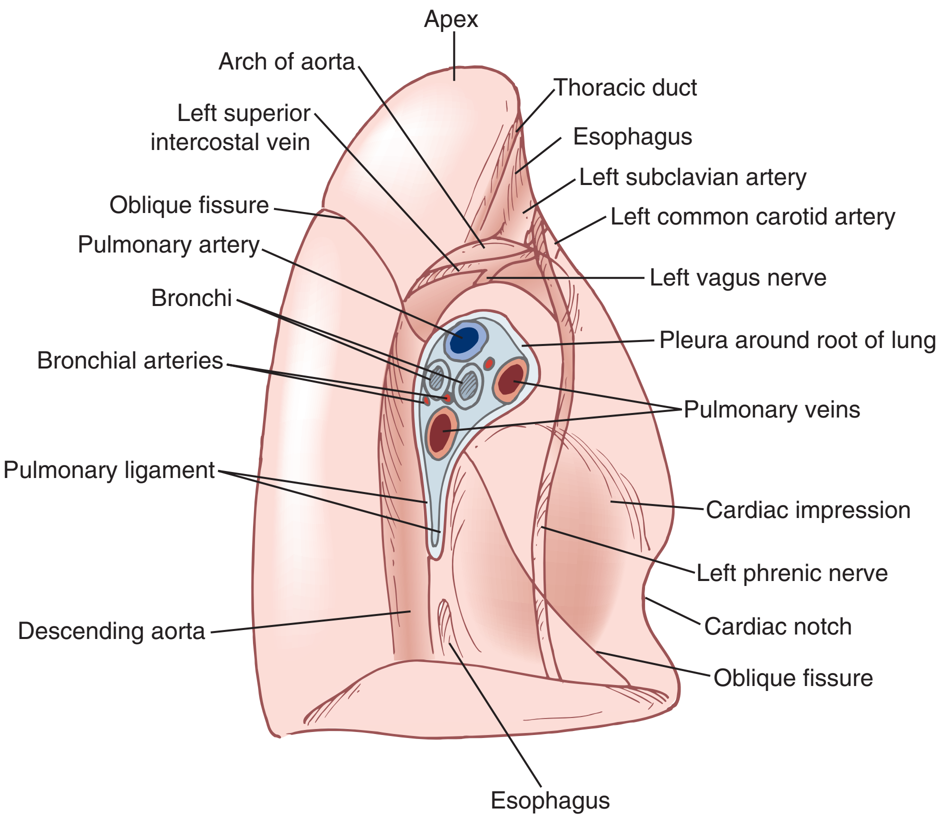

FIGURE 1-14 ■ The medial surface of the left lung.

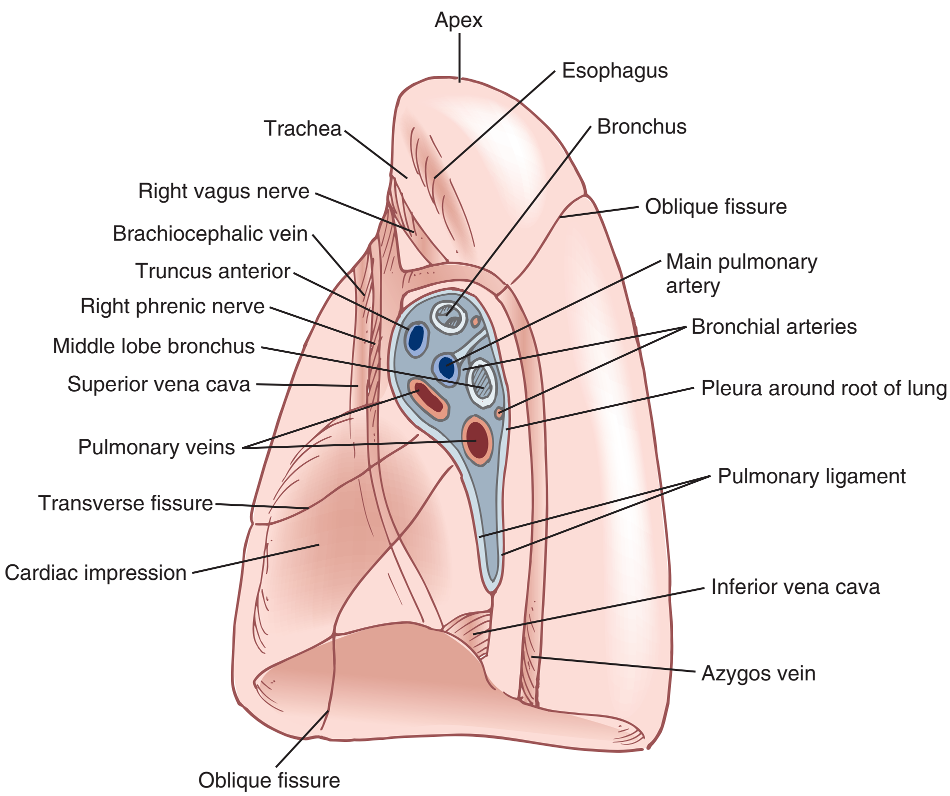

FIGURE 1-15 ■ The medial surface of the right lung.

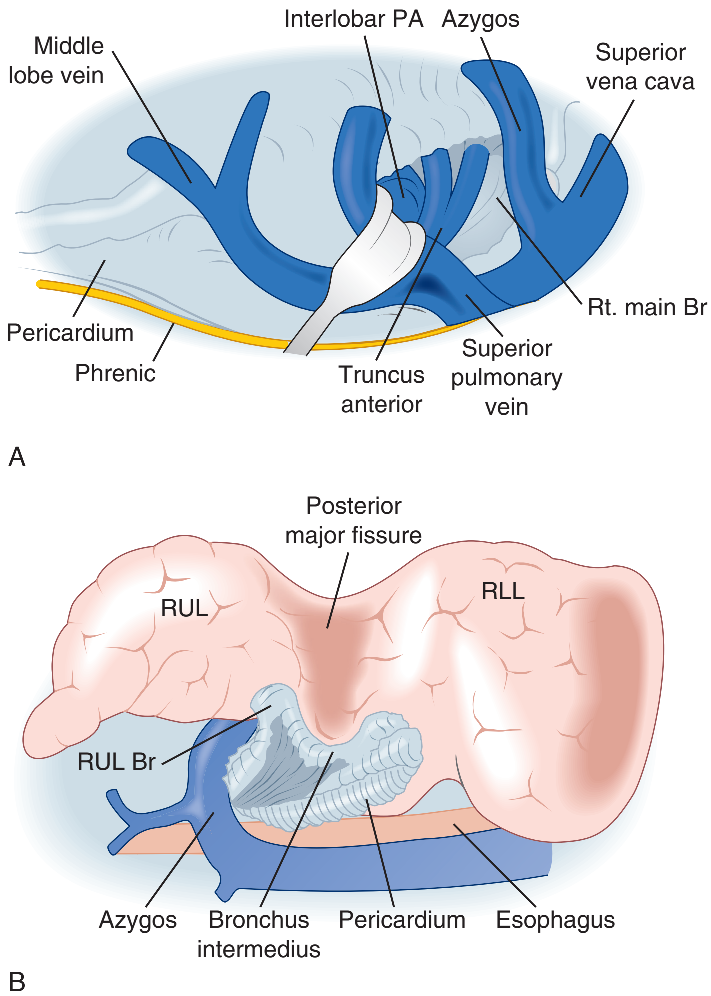

FIGURE 1-16 ■ Hilum of the right lung. **A,** Anterior view. **B,** Posterior view. *Br,* Branch; *PA,* pulmonary artery; *RLL,* right lower lobe; *RUL,* right upper lobe.

enters the lung hilum (Fig. 1-16). The interlobar pulmonary artery goes between the bronchus intermedius (posterior) and superior pulmonary vein (anteriorly) and gives off the posterior ascending artery to the posterior segment of the upper lobe (Fig. 1-17). The ongoing pulmonary artery then runs behind the middle lobe bronchus. Opposite the posterior ascending artery, the middle lobe artery arises anteromedially, usually at the junction of the horizontal and oblique fissures. The arterial branch to the superior segment of the lower lobe arises posteriorly and opposite the middle lobe artery at the same level or slightly distal to it. Beyond the superior segmental artery, the common basal trunk continues in the fissure to give rise to the medial basal segmental artery, occasionally as a common branch with the anterior basal branch. The terminal branches supply the lateral and posterior basal segments.

The left pulmonary artery passes more posteriorly and superiorly than the right and is longer before giving off its first branch. Commonly, there are four branches to the left upper lobe, but the number varies from two to seven. The first branch arises from the anterior portion of the artery and is quite short, and often its branches

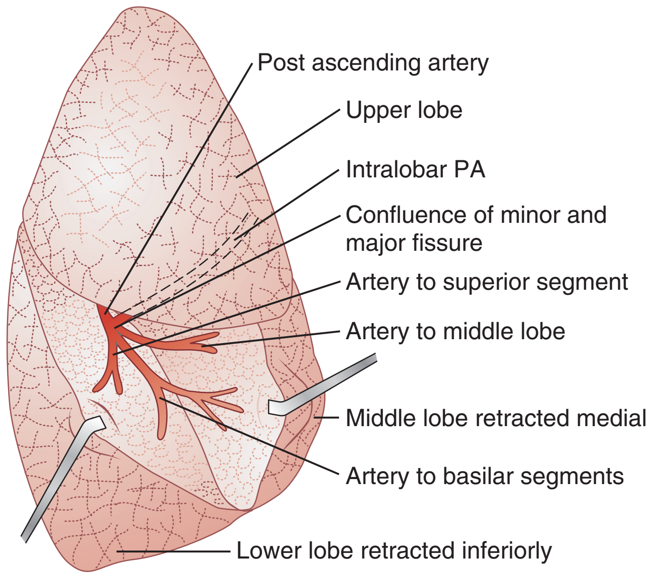

FIGURE 1-17 ■ Pulmonary artery as it exits the parenchyma of the right upper lobe into the confluence of the major and minor fissures. *PA,* Pulmonary artery.

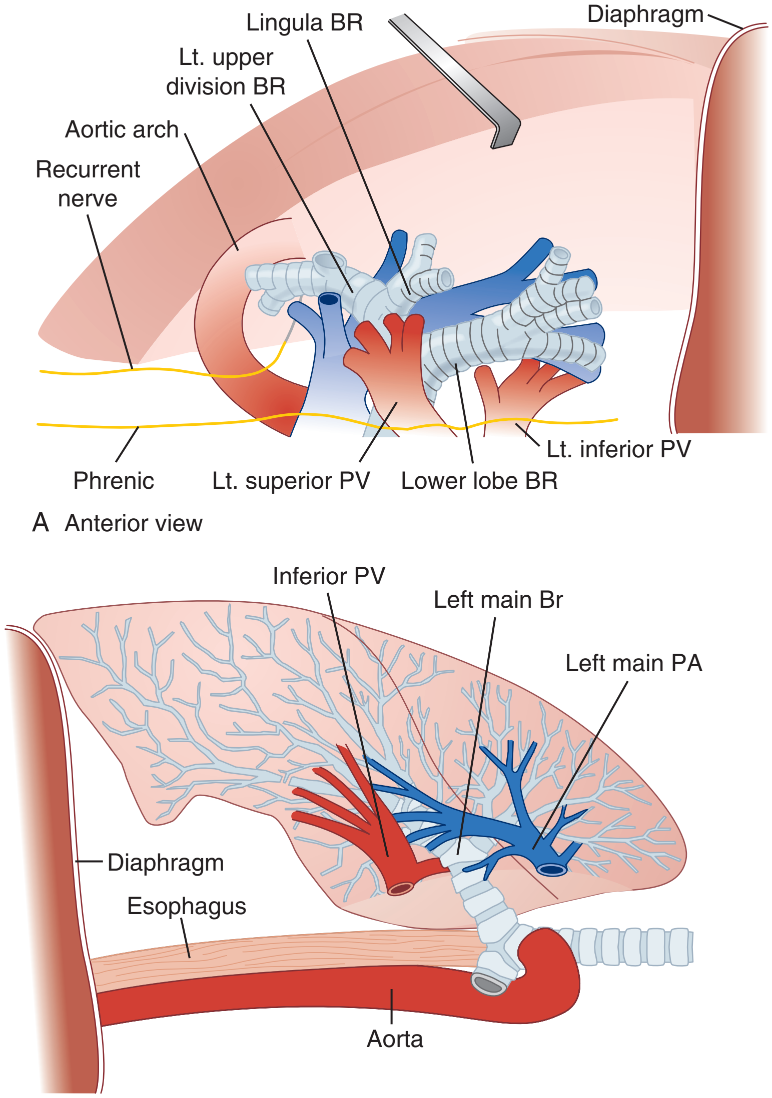

FIGURE 1-18 ■ Hilum of the left lung. **A,** Anterior view. **B,** Posterior view. *BR,* Branch; *Lt.,* left; *PA,* pulmonary artery; *PV,* pulmonary vein.

appear as separate vessels arising from the main artery. The second branch usually arises posterosuperiorly as the main artery passes over the left upper lobe bronchus and into the interlobar fissure, where more ascending upper lobe branches may originate (Fig. 1-18). As it enters the interlobar fissure, it gives off a branch to the superior segment of the left lower lobe and the lingular artery. Beyond the lingular branch, the common basal trunk divides into two major branches. The anterior branch supplies the anteromedial basal segments and the posterior branch supplies the lateral basal segments.

Among the common variations of the pulmonary arterial supply, the first anterior trunk on the left may be the major supply to the lingular segments. This should be suspected if a small lingular artery is found in the anterior fissure. The right side may have two major arteries that arise from the truncus anterior, which are designated the truncus anterior superior and the truncus anterior inferior.

The left superior pulmonary vein receives all the tributaries from the left upper lobe. It is closely applied to the anteroinferior portion of the pulmonary artery and makes dissection of the anterior branches quite hazardous. Its three main tributaries are apical posterior, anterior, and lingular. Occasionally, the superior and inferior lingular veins are separate. A common anomaly is drainage of the inferior lingular vein into the inferior pulmonary vein. The inferior pulmonary vein, lying more posteriorly and inferiorly, drains the entire lower lobe via two principal tributaries, the superior segmental and common basal veins. The right superior pulmonary vein is usually made up of four branches: the apical anterior, anterior-inferior, and posterior branches, which drain the upper lobe, and the inferior branch, which drains the middle lobe. Occasionally, the middle lobe vein drains into the atrium as a separate vessel and very rarely it becomes a tributary of the inferior pulmonary vein.

The right inferior pulmonary vein is similar to the one on the left and is composed of two trunks. The common basal vein is composed of the superior basal and inferior basal tributaries, and the superior segmental vein drains the superior segment of the lower lobe. The superior and inferior pulmonary veins on the right most often enter the left atrium separately. In contrast, on the left, the two veins form a common trunk in more than 25% of the population.

The segmental branches of the pulmonary arteries usually lie on the superior or lateral surface of the segmental bronchus that they accompany and with which they branch. The venous tributaries occupy an intersegmental position, do not bear as close a relationship to the segmental bronchi, and tend to lie on their medial or inferior surfaces. Variations from the usual pattern are common. As a general rule, veins vary more than arteries, and arteries vary more than bronchi.

The systemic circulation of the lung tissues is derived from the bronchial arteries that supply the bronchi from the carina to their terminal bronchioles and that also nourish the connective tissue and visceral pleura. A single right bronchial artery usually branches from the third posterior intercostal artery, and two left bronchial arteries usually branch from the dorsal aorta, one near vertebra T5 and one inferior to the left principal bronchus. Although variations are known, most bronchial arteries arise from the anterolateral aspect of the aorta or its branches within 2 to 3 cm of the origin of the left subclavian artery and come to lie on the membranous portion of the principal bronchi. The bronchial arteries usually give off branches to the esophagus and then follow the bronchi into the lung, also giving off branches along the interalveolar connective tissue septae to the visceral pleura. There is a rich anastomosis with the pulmonary arterial supply, which is important after pulmonary transplantation.

The bronchial veins have a superficial system, with two bronchial veins on each side draining from the hilar region and visceral pleura into the azygos vein on the right and the accessory hemiazygos vein on the left. Most of the venous drainage from the deeper lung substance drains into the pulmonary venous system, accounting for the less than 100% saturation of the blood in the left atrium.

Lymphatic drainage channels run toward the hilum from subpleural vessels along the bronchi and pulmonary arteries. This flow is interrupted by multiple lymph nodes along the way, mostly situated at forking points of the bronchi. Each nodal station has a number assigned to it and is the basis of the most recent staging system for primary bronchogenic carcinoma, as proposed by Mountain and Dressler in 1997.

The most peripheral pulmonary nodes include subsegmental lymph nodes (level 14) and segmental (level 13), lobar (level 12), and interlobar (level 11) nodes in the fissures, and they are reliably removed during a lobectomy. The hilar lymph nodes (level 10), also known as *bronchopulmonary nodes*, are at the root of the lung and can be accessed using thoracoscopy or thoracotomy. The inferior pulmonary ligament nodes (level 9) lie in the inferior pulmonary ligament on the left and the right, and the paraesophageal nodes (level 8) lie dorsal to the posterior wall of the trachea and inferior to the carina, to the right or left of the midline esophagus (Fig. 1-19). From then onward, drainage is to the central mediastinal and tracheobronchial nodes and upward via mediastinal lymph trunks to the brachiocephalic veins (see Fig. 1-19*A*).

The right and left paratracheal lymph nodes (levels 2R and 2L), and the lower paratracheal lymph nodes at the tracheobronchial angle (levels 4R and 4L), and the subcarinal (level 7) lymph nodes can be identified and sampled via a standard cervical mediastinoscopy. During a right VATS or right thoracotomy, lymph nodes at levels 4R, 7, 8, and 9 can be sampled (see Fig. 1-19*C* and *E*). The Chamberlain procedure or the left VATS procedure can give access to the subaortic (level 5) and para-aortic (level 6) lymph nodes. Left VATS can also provide access to lymph nodes at levels 7, 8, and 9 (see Fig. 1-19*B* and *D*). The Delphian lymph node (the highest mediastinal, pretracheal lymph node) is classified as level 1.

Thus, levels 1 through 9 are considered mediastinal lymph nodes, and metastases are classified as N2 if ipsilateral and as N3 if contralateral spread of cancer is present in these lymph node stations. Anomalies of this ipsilateral, centrally directed drainage pattern are common and are more likely on the left side, especially with lower lobe tumors. Up to 50% of left lower lobe tumors and 35% of left upper lobe tumors have positive contralateral (N3) mediastinal nodes, whereas contralateral metastasis is found in only 42% of right lower lobe tumors and 18% of right upper lobe tumors when N2 lymph nodes are negative for tumor. Instead of draining to hilar nodes, the left upper lobe tumors follow an alternative path to the subaortic, periaortic, and anterior mediastinal nodes in up to one third of patients.

The vagus nerve and the sympathetic plexus contribute to the poorly developed anterior pulmonary plexus around the main pulmonary arteries, and to the well-developed posterior plexus of nerves around the bronchi. The vagus nerve carries all the afferent innervation from the bronchial mucosa, sensing stretch in the alveoli and pleura, pressure in the pulmonary veins, and mediating pain. Efferent fibers in the vagus constrict the bronchi, and the sympathetic efferents are vasoconstricting to the pulmonary vessels and secretomotor to the bronchial plexus.

The left and right hemithoraces each contain a variety of other vital organs in addition to the lungs. The thoracic duct, esophagus, aorta, and azygos vein can be visualized in the right hemithorax, whereas the aortic arch, descending aorta, and distal esophagus may be seen in the left hemithorax.

ESOPHAGUS

The esophagus is a muscular tube that starts at the upper esophageal sphincter (the cricopharyngeus) and travels approximately 25 cm to the lower esophageal sphincter at the gastroesophageal junction. The cricopharyngeus is 15 cm from the incisor teeth. With endoscopy, the gastroesophageal junction is measured to be 38 to 40 cm from the incisors in men, and generally 2 cm shorter in women. The cervical esophagus is slightly left of midline as it enters the thoracic inlet in front of the body of the T1 vertebra and posterior to the trachea. After it passes the aortic arch, it inclines forward and passes in front of the descending thoracic aorta to obtain a position left of midline as it travels through the esophageal hiatus

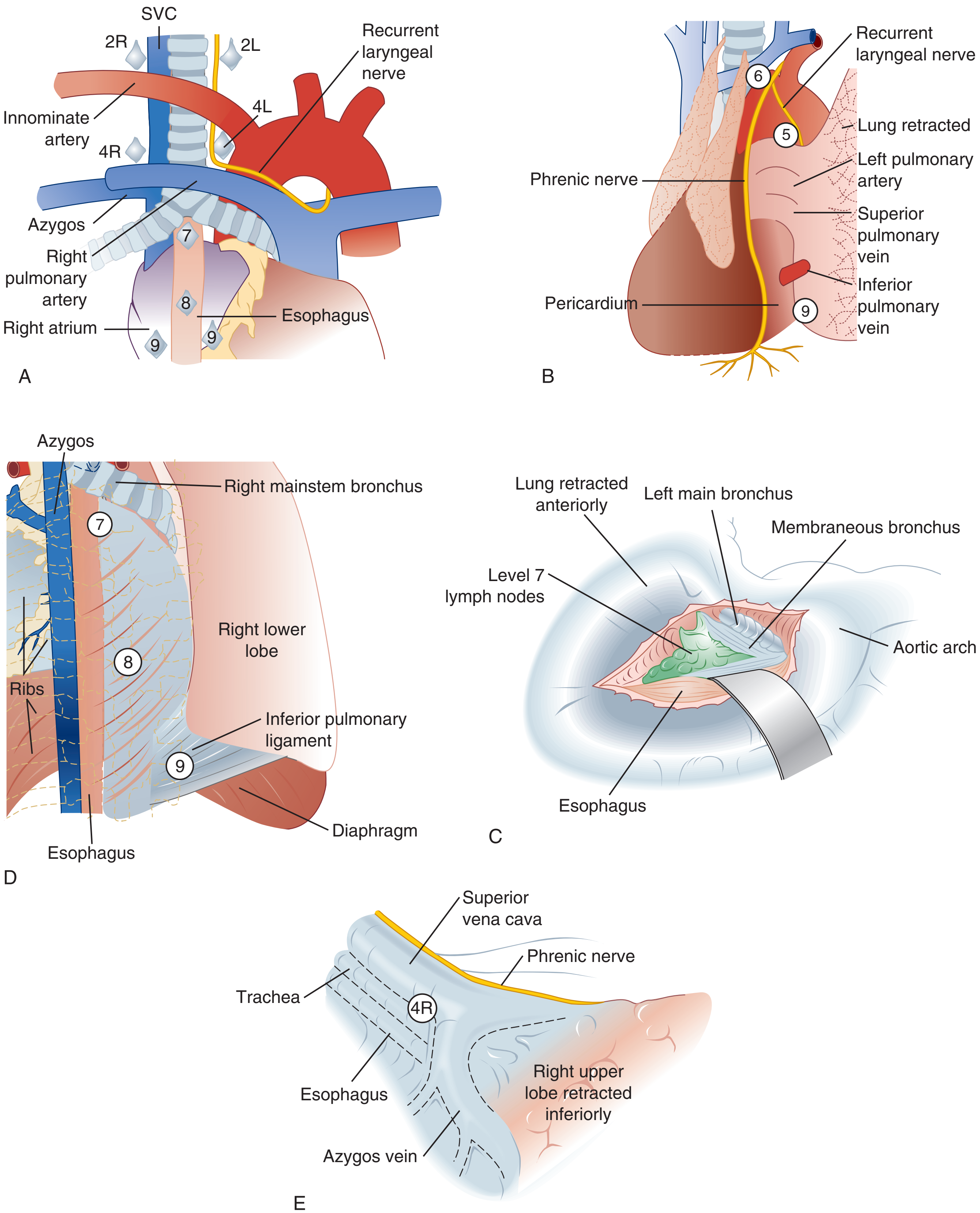

FIGURE 1-19 ■ Mediastinal lymph nodes. **A,** Anterior view. **B,** Left lung retracted posteriorly to expose lymph nodes at levels 5, 6, and 9. **C,** Anterior retraction of the left lung to expose lymph nodes at level 7. **D,** Anterior retraction of right lung to expose lymph nodes at levels 7, 8, and 9. **E,** Inferior and posterior retraction of right lung to expose lymph nodes at level 4R. *SVC,* Superior vena cava.

opposite the body of the 10th thoracic vertebra. At the level of the T8 vertebra, the left lateral wall of the esophagus that was covered by the aorta is in contact with the parietal pleura as the aorta goes directly behind it. This is a common site of perforation in patients with Boerhaave syndrome. The right lateral surface of the esophagus is completely covered by parietal pleura except where the azygos vein crosses it at the level of the T4 vertebra. When choosing the side for a thoracotomy, avoiding interference from the aortic arch is the primary concern. Access to the proximal esophagus is difficult from the left hemithorax because of the overlying aortic arch.

Endoscopic examination of the esophagus reveals several constrictions on the esophageal lumen in addition to the narrowing at the upper and lower esophageal sphincters. The additional constrictions are seen endoscopically where the esophagus crosses the aortic arch at 22 to 25 cm from the incisors, and where it is crossed by the left main-stem bronchi at 27.5 cm from the incisors. These anatomic relationships may also be seen radiographically. A notch indentation is often seen in its left lateral wall on a barium swallow radiograph as the esophagus passes to the right of the aorta at the level of the tracheal bifurcation. The left main-stem bronchus may indent it slightly as it passes over the esophagus.

The blood supply of the cervical esophagus is from branches of the inferior thyroid artery. The thoracic esophagus is supplied by the esophageal branches of the aorta and the bronchial arteries. Most individuals have one right-sided and one or two left-sided bronchial arterial branches. The upper aortic esophageal branch is usually shorter and originates at the T6 or T7 vertebral level, and the lower larger branch originates at the level of the eighth or ninth thoracic vertebra. Finally, the abdominal esophagus receives its supply from branches of the left gastric and inferior phrenic arteries. In the wall of the esophagus, there is an extensive longitudinal anastomotic network in the muscular and submucosal layers, a basis for portasystemic anastomoses. The venous drainage follows the arterial supply. A submucosal plexus drains into a periesophageal venous plexus, from which the veins originate and empty into the inferior thyroid, bronchial, azygos, and left gastric veins.

Two large interconnecting networks that course longitudinally form the lymphatic network of the esophagus. The mucosal network extends into the submucosal network, and flow is predominantly (6 : 1) longitudinal rather than segmental. These pierce the muscular wall, and ultimately lymph channels follow the arterial supply. The cervical esophagus drains into the deep cervical nodes alongside the inferior thyroid vessels, whereas the abdominal portion drains to the preaortic group of the celiac nodes along the left gastric artery. The thoracic esophagus drains into the tracheobronchial nodes superiorly and the subcarinal and paraesophageal nodes inferiorly.

After giving off their recurrent laryngeal branches, which supply the cricopharyngeal sphincter and cervical esophagus, the vagus nerves descend onto the anterior wall of the esophagus and form a complex vagal esophageal plexus, a network of interconnecting fibers that forms the preganglionic parasympathetic supply to the esophagus. These fibers connect to the enteric ganglia in the myenteric and submucosal plexuses that are located in the wall of the esophagus. Just above the diaphragm, the plexus usually gives rise to two nerve trunks: the anterior and posterior vagal. The anterior trunk contains predominantly left vagal fibers and the posterior contains mainly right, with considerable contribution from one another.

Cervical and thoracic sympathetic ganglia contribute visceral branches to the esophagus, and a few branches from the splanchnic nerves reach the esophagus. Their effect on the esophageal muscle is unknown. The vagus nerve is the motor supply to the esophageal muscle, and the secretomotor nerve supplies the esophageal glands. Afferent pain fibers appear to run in both the vagal and vasomotor sympathetic supply; hence, esophageal pain can be referred to the neck, arm, and thoracic wall.

The mucosal lining of the esophagus is composed of nonkeratinized, stratified squamous epithelium supported by a lamina propria and a thick muscularis mucosa. The mucous membrane is thick and in the collapsed state is thrown into longitudinal folds. Mucosal glands in the submucosa are mainly found at the upper and lower ends of the esophagus. The muscular wall consists of an inner circular and an outer longitudinal layer that are visceral smooth muscle in the lower two thirds and skeletal striated muscle in the upper third. Except for the short intra-abdominal segment, the lack of a serosa in the rest of the esophagus accounts for the difficulty in suturing the esophagus.

VESSELS OF THE THORAX

Descending Thoracic Aorta

The descending thoracic aorta starts at the level of the fourth thoracic vertebra. It is a posterior mediastinal structure that arises just left of the vertebral column and travels toward the midline as it descends toward the diaphragm. When it goes through the aortic hiatus at the level of the 12th thoracic vertebra, it is anterior to the vertebral column. In the left hemithorax, anterior to the descending aorta, are the left pulmonary hilum, the pericardium, and the esophagus, and posteriorly is the vertebral column. In the right hemithorax, the esophagus is lateral to the aorta until it takes up a position anterior to the aorta near the diaphragm. The thoracic duct and azygos vein are lateral to the aorta in the right hemithorax. Branches of the descending thoracic aorta include pericardial, bronchial, mediastinal, phrenic, and posterior intercostal and subcostal arteries. The descending aorta is fixed at the origin of the left subclavian artery, which is therefore a common site for transection of the aorta during motor vehicle accidents.

Azygos Vein

The origin of the azygos vein is not constant. It typically starts from the posterior aspect of the inferior vena cava, but it may originate from a lumbar azygos vein or from the confluence of the subcostal and ascending lumbar vein. It ascends through the aortic hiatus in the diaphragm. It rises in the right hemithorax in the posterior mediastinum until the fourth vertebral body, and then it turns medially over the right pulmonary hilum to join the superior vena cava.

Thoracic Duct

The thoracic duct carries chylous material, which is rich in lipids, proteins, and lymphocytes. It begins at the confluence of the abdominal lymphatic trunks known as the cisterna chili. From its origin at the level of the 12th thoracic vertebra, the thoracic duct travels through the aortic hiatus and ascends in the right hemithorax between the descending thoracic aorta (medial) and the azygos vein (lateral) and posterior to the esophagus, until it crosses medially at the level of the fifth thoracic vertebral body. Once in the left hemithorax, it continues its ascent on the left side of the esophagus. It crosses the aortic arch anteriorly and then travels posterior to the left subclavian artery. It travels out of the thoracic inlet for 3 to 4 cm before arching and descending anterior to the medial border of the scalenus anterior and finally joining the venous system near the confluence of the left subclavian and internal jugular veins.

NERVES OF THE THORAX

Vagus and Recurrent Laryngeal Nerves

The vagus nerve passes inferiorly from the base of the skull to the thoracic inlet in the carotid sheath. On the right side, the right vagus travels behind the internal jugular vein and dives behind the sternoclavicular joint to give off the right recurrent laryngeal nerve. The right recurrent laryngeal nerve recurs on the ipsilateral subclavian artery and then ascends in the tracheoesophageal groove. The left recurrent laryngeal nerve recurs on the aortic arch and then rises in the tracheoesophageal groove. Both recurrent laryngeal nerves enter the larynx with the laryngeal branch of the inferior thyroid artery.

The right vagus continues to descend into the thoracic cavity behind the right brachiocephalic vein and then lateral to the trachea. It travels posteriorly and lies predominantly posterior to the right pulmonary hilum, where several bronchial branches are given off. The remaining vagal fibers join fibers from the left to form the posterior vagal trunk.

The left vagus enters the thorax between the common carotid and the subclavian arteries behind the left brachiocephalic vein. It crosses the left side of the aortic arch and gives off the left recurrent laryngeal nerve before descending behind the left pulmonary hilum. It also gives off bronchial branches at this level. Fibers from the left and right vagi form the anterior and posterior vagal trunks, which enter the abdomen through the esophageal hiatus.

Thoracic Sympathetic Chain

The thoracic sympathetic chain is formed by ganglia of the autonomic nervous system. The first thoracic ganglia, in the majority of patients, fuses with the inferior cervical ganglia. The thoracic sympathetic chain predominantly lies on the costal head under the pleura. The nerves interact with corresponding spinal nerves with white and gray rami. Ligation of sympathetic ganglia is performed to treat hyperhidrosis, facial blushing, Raynaud disease, and reflex sympathetic dystrophy. When collateral nerve fibers bypass the sympathetic trunk, sympathectomy results in failure. These fibers can reach the brachial plexus without passing through the sympathetic ganglia. The nerve of Kuntz is the most described collateral nerve. Although in clinical literature, the nerve of Kuntz is reported in 10% of cases, it is reported 80% of the time in anatomic descriptions. Techniques for ligation of ganglia from T1 to T3 are discussed in later chapters.

Phrenic Nerves

The right and left phrenic nerves arise from the third, fourth, and fifth cervical rami and course inferiorly in an oblique manner on the respective anterior surfaces of the scalenus anterior muscle. At the thoracic inlet, the nerve is on the medial border of the scalenus anterior muscle, just 3 to 4 cm from the sternoclavicular joint. It then enters the thoracic inlet posterior to the subclavian vein and anterior to the internal mammary artery. Injury to the phrenic nerve may occur during surgical procedures such as a scalene node biopsy or Pancoast tumor resection. When dissecting a pre-scalene node, which is often done for lung cancer staging or confirmation of sarcoidosis, caution should be used to avoid entering the scalenus anterior sheath in which the phrenic nerve lies. Pancoast tumor resections require division of the first rib. The scalenus anterior muscle should be divided as close to the first rib as possible to avoid injury to the overlying phrenic nerve.

After entering the thoracic cavity, the right phrenic nerve travels inferiorly, just lateral to the brachiocephalic vein and the superior vena cava. It continues its descent over the pericardium and the underlying right atrium and inferior vena cava. Just as it goes through the diaphragm, it divides into three branches: the anterior, posterior, and anterolateral.

The left phrenic nerve at the root of the neck may pass anterior to the first part of the subclavian artery and behind the thoracic duct, or it may follow the same course as the right phrenic nerve. It then crosses anterior to the internal mammary artery and travels in the groove between the left common carotid and subclavian arteries. The nerve crosses anteromedial to the aortic arch and travels over the pericardium toward the diaphragm. In the same manner as its right-sided counterpart, the nerve divides as it travels through the diaphragm to give off branches on the abdominal surface. The branches travel from its central position in the diaphragm to supply the sternal, crural, and posterior aspects of the diaphragm. Radial incisions in the diaphragm from the costal edge to the esophagus will lead to damage of the phrenic nerve. Peripheral circumferential incisions in the diaphragm are safest with regard to the phrenic nerve. Similar incisions in the central tendon are also safe.

SUGGESTED READINGS

Agur AMR, Lee MJ: *Grant's atlas of anatomy*, ed 10, Philadelphia, 1999, Lippincott Williams & Wilkins.

Bannister LH, Berry MM, Collins P, et al: *Gray's anatomy: the anatomical basis of medicine and surgery*, ed 38, New York, 1995, Churchill Livingstone.

Brock RC: *The anatomy of the bronchial tree: with special reference to the surgery of lung abscess*, ed 2, London, 1954, Oxford University Press.

Butler J: *The bronchial circulation; lung biology in health and disease*, *vol* 57, New York, 1992, Marcel Dekker.

Butler P, Mitchell AWM, Ellis H: *Applied radiological anatomy*, Cambridge, UK, 1999, Cambridge University Press.

Cho DM, Lee DY, Sung SW: Anatomical variations of rami communicantes in the upper thoracic sympathetic trunk. *Eur J Cardiothorac Surg* 27:320–324, 2005.

Chung IH, Oh CS, Koh KS, et al: Anatomical variations of the T2 nerve root (including the nerve of Kuntz) and their implications for sympathectomy. *J Thorac Cardiovasc Surg* 123:498–501, 2002.

Clemente CD: *Gray's anatomy*, American ed 30, Philadelphia, 1985, Lea & Febiger.

Conley DM, Rosse C: *The digital anatomist: the interactive atlas of thoracic viscera (CD-ROM)*, Seattle, 1996, University of Washington School of Medicine.

Deslauriers J: Thoracic anatomy part I. *Thorac Surg Clin* 17:443–666, 2007.

Ehrlich E, Alexander WF: Surgical implications of upper thoracic independent sympathetic pathways. *Arch Surg* 62:6009–6014, 1951.

Funatsu T, Yoshito M, Hatakenoka R, et al: The role of mediastinoscopic biopsy in preoperative assessment of lung cancer. *J Thorac Cardiovasc Surg* 104:1688, 1992.

Hashmonai M, Kopelman D, Kein O, et al: Upper thoracic sympathectomy for primary palmar hyperhidrosis: long-term follow-up. *Br J Surg* 79:268–271, 1992.

Healy JE: *Surgical anatomy of the thorax*, Philadelphia, 1970, WB Saunders.

Jackson CL, Huber JF: Correlated applied anatomy of the bronchial tree and lungs with a system of nomenclature. *Dis Chest* 9:319, 1943.

Kirgis HD, Kuntz A: Inconstant sympathetic neural pathways: their relation to sympathetic denervation of the upper extremity. *Arch Surg* 44:95–102, 1942.

Kuntz A: Distribution of the sympathetic rami to the brachial plexus: its relation to sympathectomy affecting the upper extremity. *Arch Surg* 15:871–877, 1927.

Lewis WH: *Gray's anatomy: the anatomical basis of medicine and surgery*, ed 20, New York, 2000, Bartleby.

Liebow AA: Patterns of origin and distribution of the major bronchial arteries in man. *Am J Anat* 117:19, 1965.

Lin TS: Video-assisted thoracoscopic "resympathicotomy" for palmar hyperhidrosis: analysis of 42 cases. *Ann Thorac Surg* 72:895–898, 2001.

Marhold F, Izay B, Zacherl J, et al: Thoracoscopic and anatomic landmarks of Kuntz's nerve: implications for sympathetic surgery. *Ann Thorac Surg* 86:1653–1658, 2008.

Marhold F, Neumayer C, Tschabitscher M: The sympathetic trunk and its neural pathway to the upper limb: review of the literature. *Eur Surg* 37:114–120, 2005.

Medlar EM: Variations in interlobar fissures. *Am J Roentgenol* 57:723–725, 1947.

Mountain CF, Dressler CM: Regional lymph node classification for lung cancer staging. *Chest* 111:1718, 1997.

Netter FM: *The Ciba collection of medical illustrations*, *vol* 7, Summit, NJ, 1996, Ciba-Geigy.

Ramsaroop L, Partab P, Singh B, et al: Thoracic origin of a sympathetic supply to the upper limb: the "nerve of Kuntz" revisited. *J Anat* 199:675–682, 2001.

Ramsaroop L, Singh B, Moodley J, et al: Anatomical basis for a successful upper limb sympathectomy in the thoracoscopic era. *Clin Anat* 17:294–299, 2004.

Riquet M, Manach D, Dupont P, et al: Anatomic basis of lymphatic spread of lung carcinoma to the mediastinum: anatomo-clinical correlations. *Surg Radiol Anat* 16:229, 1994.

Rosse C, Rosse PG: *Hollinshead's textbook of anatomy*, ed 5, Philadelphia, 1997, Lippincott-Raven.

Roussos C: *The thorax; lung biology in health and disease*, *vol 85*, New York, 1995, Marcel Dekker.

Shields TW: *The mediastinum, its compartments and the mediastinal lymph nodes. General thoracic surgery*, ed 5, Philadelphia, 2000, Lippincott Williams & Wilkins.

Van Rhede van der Kloot E, Drukker J, Lemmens HAJ, et al: The high thoracic sympathetic nerve system—its anatomic variability. *J Surg Res* 40:112–119, 1986.

Wragg LE, Milloy FJ, Anson BJ: Surgical aspects of the pulmonary artery supply to the middle lobe and lower lobes of the lungs. *Surg Gynecol Obstet* 127:531, 1968.

CHAPTER 2

Radiologic Imaging of Thoracic Abnormalities

Jeremy J. Erasmus • Edith M. Marom • Tam T. Huynh • Edward F. Patz, Jr.

CHAPTER OUTLINE

Since the late 1990s advances in imaging technology, including digital subtraction chest radiographs, multidetector spiral computed tomography (MDCT), dual-energy computed tomography (CT) techniques, electrocardiograph (ECG)-gated CT, positron emission tomography (PET) with CT, and magnetic resonance imaging (MRI), have improved diagnostic accuracy and management of patients with thoracic abnormalities. The electronic distribution of these studies as digital images via a picture archiving and communication system, has also expedited information transfer and interpretation.

This chapter is a general overview of the advances in thoracic imaging, with a focus on imaging modalities used for the evaluation of the surgical patient. Topics reviewed include a spectrum of mediastinal, lung, pleural, and chest wall abnormalities commonly encountered by thoracic surgeons in which imaging is important in the diagnosis and management of patients.

MEDIASTINAL ABNORMALITIES

Mediastinal abnormalities have a variety of causes, including congenital malformations, infections, trauma, and neoplasms. Clinical history and prior radiographs are often sufficient to determine the cause and the necessity for further evaluation. In the absence of prior imaging studies, chest radiographs, CT, or MRI are most commonly used to establish a diagnosis or to provide a differential diagnosis.

Aorta

Multidetector computed tomography, dual-energy CT, and ECG-gated CT together with sophisticated post-processing methods have transformed imaging of the thoracic aorta. More recently, rapidly acquired (single breath-hold) non–ECG-gated CT imaging has become available and is being used as the initial diagnostic imaging modality to evaluate patients with suspected acute aortic dissection. Furthermore, because single-acquisition dual-source CT with the availability of low- and high-kVp data acquired from the same volume eliminates aortic precontrast imaging, reduces radiation exposure, and uniquely characterizes aortic pathology, it is being recommended in the initial evaluation of the aorta.

Aortic Dissection

Acute aortic syndrome is the term currently used to refer to a group of potentially life-threatening disorders of the thoracic aorta including aortic dissection, intramural hematoma (IMH), and penetrating atheromatous ulcer (PAU).[1] The most common presenting complaint in patients with acute aortic syndrome is acute onset of severe chest pain, but symptoms can be nonspecific and variable.[1,2] Aortic dissection is the most common acute aortic disorder, and IMH and PAU account for 10% to 20% of acute aortic syndrome cases.[2,3] Two different mechanisms leading to the characteristic intimal tear in aortic dissection have been proposed and remain

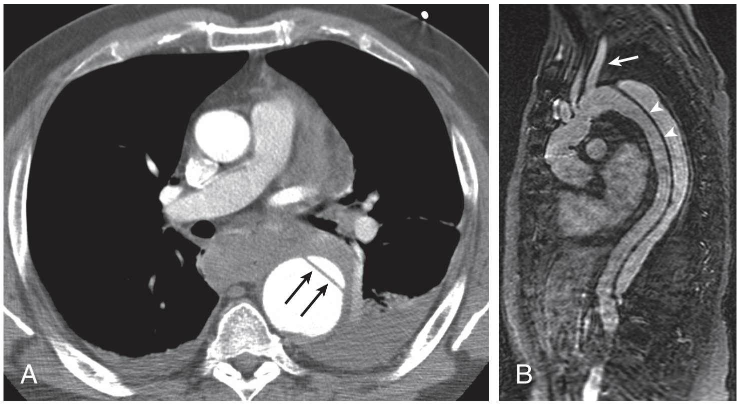

FIGURE 2-1 ■ Type B aortic dissection. **A,** Axial contrast-enhanced chest computed tomography shows a dilated descending aorta and an intimal flap *(arrows)*. There are small pleural effusions and increased attenuation of mediastinal adipose tissue raising the possibility of hemorrhage within the mediastinum. **B,** Sagittal oblique magnetic resonance imaging of the aorta shows an intimal flap *(arrowheads)* arising distal to the left subclavian artery *(arrow)*.

debatable: primary disruption of the intima versus secondary rupture of a hematoma arising from the vasa vasorum.[4,5]

MDCT with intravenous contrast is the imaging modality of choice when an aortic dissection is suspected, and it can determine the type and extent of the dissection for management decisions. The DeBakey and Stanford classifications are widely recognized and both based on the origin of the intimal tear and the extent of the aortic involvement. Stanford Type A dissection involves the ascending aorta and originates just above the aortic valve plane; it is usually considered for surgical repair. Stanford Type B dissection originates just below the level of the ligamentum arteriosum, and it is generally managed medically. Endovascular or surgical interventions are indicated for patients who develop complications from Stanford Type B dissections (Fig. 2-1).

The primary diagnostic finding on CT is an intimal flap separating the true from the false lumen. The sensitivity and specificity approaches 100%, with an accuracy that is superior to that of angiography.[6-8] Images are usually viewed as two-dimensional orthogonal axial sections, combined with volume-rendering and multiplanar reconstruction images. However, these techniques are unable to depict the dissection wall as a whole. To overcome this limitation, an automatic segmentation and three-dimensional visualization of the dissection wall has been proposed to isolate the dissection (or flap) from the rest of the vascular structures and improve diagnosis and characterization of the dissection.[9] When iodinated contrast agents are contraindicated, MRI or transesophageal echocardiography can be used to diagnose and determine the type of dissection.[10] Although these imaging modalities are accurate, both have limitations in large patients, and the ability to perform these studies in the acute setting is not optimal.

Aortic Trauma

Patients with thoracic trauma usually require imaging evaluation, and the type of study depends on the mechanism of injury and the structures potentially involved. From an imaging perspective, the chest radiograph is typically the first study performed and often dictates whether additional imaging is warranted. The radiographic findings suggestive of traumatic aortic injury (TAI) are an indistinct aortic arch or descending aorta, a left apical cap, tracheal displacement to the right, displacement of the nasogastric tube to the right of the T4 spinous process, mediastinal widening, and inferior displacement of the left main-stem bronchus (Fig. 2-2).[11-13] Less specific findings include a left pleural effusion and widening of the paravertebral stripe. These features, however, are only suggestive, not indicative, of an aortic injury. In contrast, the negative predictive value of a normal chest radiograph for an aortic injury is 94% to 96%.[14,15] If there is a chest radiographic abnormality, MDCT is the primary imaging method for the diagnosis of TAI. The sensitivity for this technique is 100%, and the specificity ranges from 83% to 99.7% (Fig. 2-3).[16-20] In fact, MDCT has superseded aortography in the

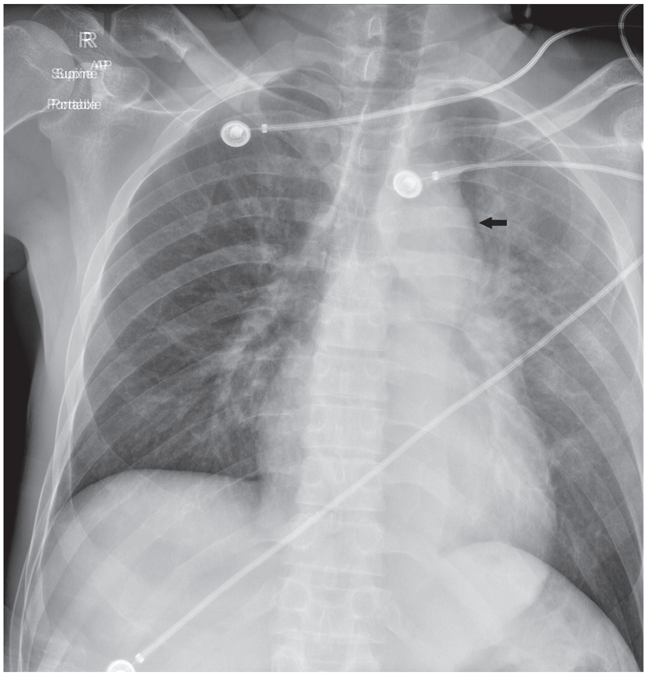

FIGURE 2-2 ■ Traumatic aortic injury. Portable chest radiograph shows widening of the superior mediastinum, lobular contour abnormality of the transverse aorta *(arrow)*, indistinct descending aorta, and opacities in the left lung consistent with pulmonary contusion/hemorrhage.

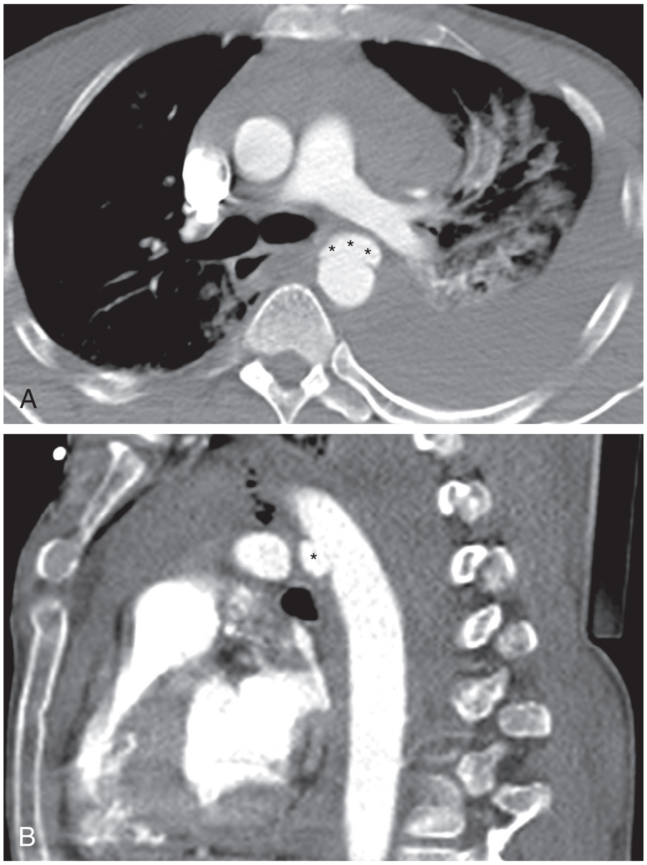

FIGURE 2-3 ■ Traumatic aortic injury after motor vehicle accident. **A,** Axial contrast-enhanced chest computed tomography (CT) shows focal contained collection of contrast *(asterisks)* located external to the descending aorta, consistent with a pseudoaneurysm. Note mediastinal widening due to hemorrhage and moderate pleural effusion. **B,** Sagittal reconstructed CT shows pseudoaneurysm arising from the thoracic aorta immediately distal to the transverse arch *(asterisk).* (Courtesy Page H. McAdams, Duke University, Durham, N.C.)

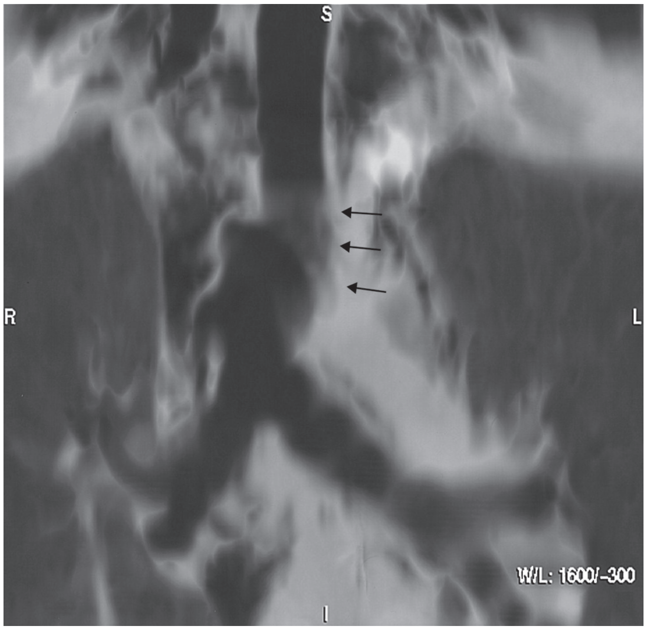

FIGURE 2-4 ■ Tracheal rupture after a motor vehicle crash in a patient with no respiratory symptoms and a chest radiograph demonstrating pneumomediastinum. Coronal reformations of computed tomography (2.5-mm collimation) show pneumomediastinum and discontinuation of the trachea *(arrows).*

diagnosis of TAI and vascular injuries and selective aortography is now reserved for therapeutic catheter-based endovascular interventions. Direct signs for TAI include a linear intraluminal filling defect, pseudoaneurysm formation, an abrupt caliber change, and contrast extravasation. Indirect signs of TAI, most notably a periaortic hematoma, are found in 91% of patients with surgically proven TAI.[17] The absence of a periaortic abnormality and a normal-appearing aorta on MDCT has a negative predictive value of 100%.[19,20] Additional nonvascular thoracic injuries can be found in 7% of patients who do not have an aortic transection on MDCT. Such abnormalities are usually a combination of pneumothoraces, multiple rib fractures, and pulmonary contusions.[17,21]

Trauma: Airways and Esophagus

Tracheal and esophageal injuries are uncommon but are typically found after intubation, a motor vehicle crash, or penetrating trauma (Fig. 2-4). Many of these injuries are not recognized initially because of subtle or nonspecific clinical and radiologic findings. Delayed or missed diagnosis can result in death or severe complications, such as ventilatory failure, mediastinitis, sepsis, airway stenosis, bronchiectasis, recurrent pulmonary infections, and permanent pulmonary function impairment.

Injuries to the trachea or bronchi can be difficult to diagnose, because patients can have no clinical findings and the radiograph can be normal in up to 10%.[22,23] In addition, the radiographic findings of tracheobronchial and esophageal injury are nonspecific and can include pneumomediastinum, pneumothorax, and progressive subcutaneous emphysema. However, diagnosis of these injuries is important because there is a high association with esophageal and major vascular injuries.[22,23] MDCT with multiplanar reconstructions is the imaging modality of choice for visualization of the airways. MDCT has a sensitivity of 85% for the detection of tracheal injuries.[22,23] Patients with tracheal rupture characteristically have an abnormal air collection in the thorax, and air can occasionally be demonstrated in the soft tissues of the neck.[22] Success in visualizing the tracheal injury ranges from 71% to 94%, and multiplanar reconstructions can be useful in localizing and defining the extent of injury.[22,24] MDCT also provides information about the esophagus, although if pneumomediastinum, with or without mediastinal fluid is present on chest radiographs or CT after trauma, fluoroscopic esophagography or endoscopy is usually warranted to exclude an esophageal tear. However, recently it has been reported that the high sensitivity and negative predictive value of CT in patients with pneumomediastinum being evaluated for esophageal perforation after trauma negates performing fluoroscopic esophagography.[25]

Evaluation of Airways: Nontrauma

Focal or diffuse lesions of the central airways are produced by a variety of diseases, including infection, malignancy, trauma, aspiration, collagen vascular disease, and idiopathic entities such as sarcoidosis or amyloidosis. Although patients might have significant symptoms, airway abnormalities are frequently not apparent or are overlooked on the chest radiograph. If there is a clinical suspicion of a tracheobronchial abnormality, further evaluation by CT is warranted. MDCT using thin slices (1 to 3 mm) is preferred, as it produces excellent axial and multiplanar images, including virtual bronchoscopy, that allow complex tracheobronchial anatomy to be visualized, depicting even weblike stenosis that can easily be missed or underestimated with thicker sections (Fig. 2-5).[26] MDCT performed during dynamic exhalation is also useful in demonstrating the excessive tracheal collapse that can occur because of either weakness of the supporting tracheal cartilaginous structures (tracheomalacia) or from excessive anterior bulging of the posterior membranous wall of the trachea (excessive dynamic airway collapse).[27,28] These related disorders are a potentially underdiagnosed cause of chronic respiratory symptoms.

Mediastinal Tumors

Mediastinal tumors, a large, diverse group of neoplasms, have historically been described radiographically according to their location in the anterior, middle, or posterior compartments. This description facilitates differential diagnosis and can aid in treatment planning.

Tumors that occur primarily in the anterior mediastinum include hemangiomas, lymphatic malformations, thymic lesions (e.g., cysts, thymolipoma, thymoma, thymic carcinoma), parathyroid adenomas, germ cell tumors, and lymphoma (Fig. 2-6). CT and MRI are particularly useful for showing local soft tissue and vascular invasion of thymomas, local invasion, and early dissemination to regional lymph nodes of thymic carcinomas and, because of the varying composition of soft tissue, fat, calcium, and hemorrhage in teratomas, can occasionally differentiate these tumors from thymomas and lymphomas.

Tumors that occur primarily in the middle mediastinum are foregut malformations, pericardial cysts, and neoplasms arising from the esophagus and trachea. Bronchogenic cysts are the most common mediastinal foregut cysts and are typically located in the subcarinal or right paratracheal region. They appear on CT as round or spherical masses of water attenuation, although many have increased attenuation from proteinaceous debris or blood.[29] Esophageal tumors can manifest as middle mediastinal masses, although esophageal carcinoma more frequently manifests as diffuse thickening of the esophagus. Endoscopy and endoscopic-directed ultrasound biopsy are usually used to evaluate locoregional extent and nodal metastases. CT is useful in showing the extent of involvement of adjacent structures such as the airways, aorta, pericardium, and spine, and in revealing nodal (e.g., celiac, gastrohepatic ligament) and systemic metastases.

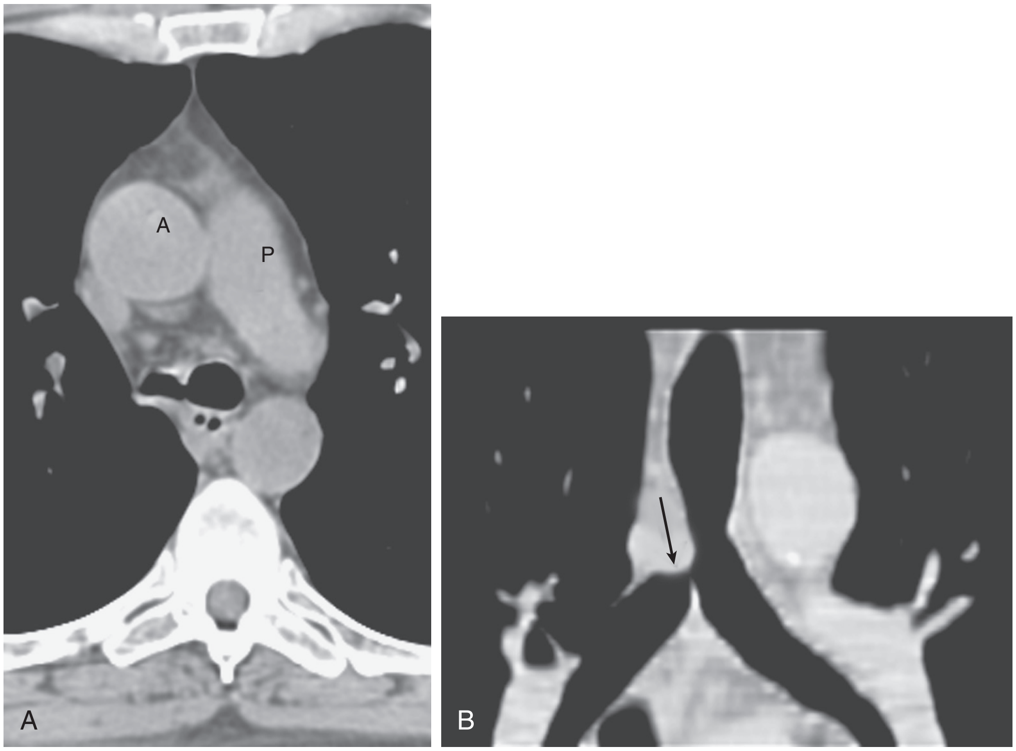

FIGURE 2-5 ■ Focal stenosis of the right main-stem bronchus from invasive aspergillosis. **A,** Axial computed tomography shows normal caliber of left main bronchus and marked concentric narrowing of right main bronchus. **B,** Coronal reconstruction shows that the right main bronchus stenosis involves a short focal segment *(arrow)*. *A,* Ascending aorta; *P,* pulmonary artery.

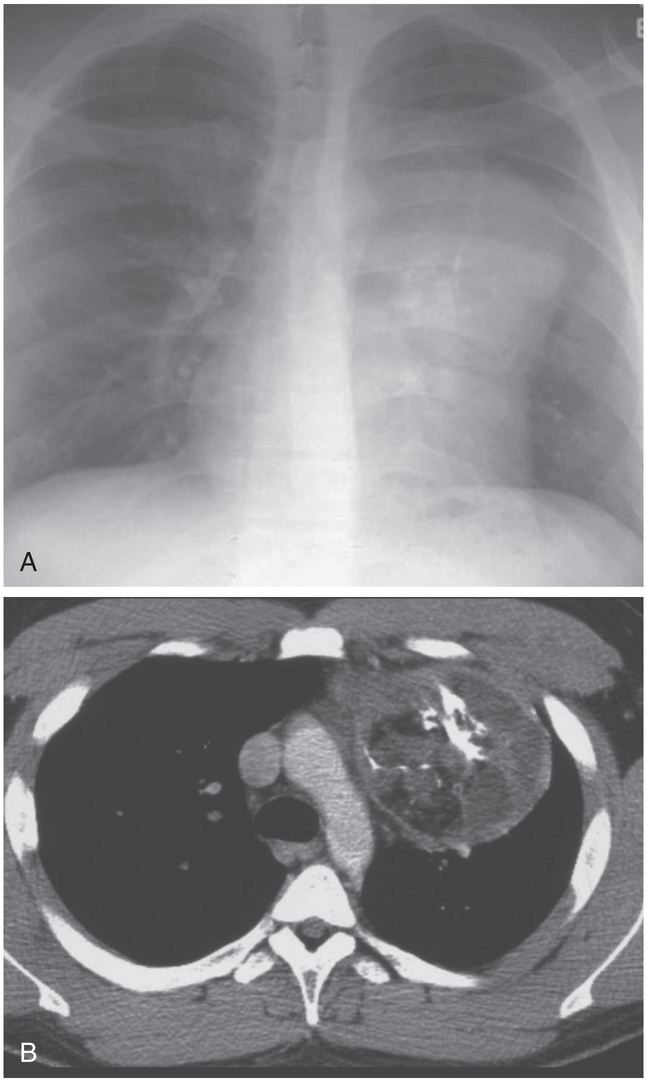

FIGURE 2-6 ■ Anterior mediastinal mass. **A,** Posteroanterior chest radiograph demonstrates a smoothly marginated, left-sided anterior mediastinal mass. **B,** Axial computed tomographic image confirms the mass, with mixed heterogeneous components, including fat, soft tissue, fluid, and calcification. These findings are diagnostic of a teratoma.

Tumors that occur primarily in the posterior compartment are neurogenic tumors. In fact, 20% of all adult and 35% of all pediatric mediastinal neoplasms are neurogenic tumors, and most are located in the posterior mediastinum.[30] Neurogenic tumors are classified as tumors of peripheral nerves (neurofibromas, schwannomas, malignant tumors of nerve sheath origin) or sympathetic ganglia (ganglioneuromas, ganglioneuroblastomas, neuroblastomas) and are optimally assessed by MRI. MRI is the preferred modality for evaluating neurogenic tumors, because it can simultaneously assess intraspinal extension, spinal cord abnormalities, longitudinal extent of tumor, and extradural extension.

LUNG ABNORMALITIES

Thoracic imaging is essential in the workup of pulmonary abnormalities, including lung nodules and focal opacities, intrathoracic malignancies, diffuse interstitial lung disease, and infection. Low-dose CT (LDCT) is being used as a screening tool for lung cancer and the National Lung Screening Trial, a randomized study comparing the effectiveness of LDCT to chest radiography in more than 50,000 participants, has reported significant reductions in lung cancer (20%) and all-cause mortality (6.7%).[31]

Solitary Pulmonary Opacities

Solitary pulmonary opacities are a common radiologic finding and are usually benign, but because of concern about lung cancer, further evaluation is often suggested. The goal is to differentiate malignant and benign lesions so that patients who require surgery are identified correctly. Although morphologic features can suggest whether a nodule is benign or malignant, there is considerable overlap, and at least 20% of malignant nodules have a benign appearance.[32,33] Specific patterns of calcification and stability in size for 2 years have historically been the only reliable findings useful in determining benignity. More recently, the ability to distinguish between benign and malignant opacities has improved with the assessment of perfusion using contrast-enhanced CT and the assessment of metabolism using PET imaging with fluorodeoxyglucose labeled with radioactive fluoride (^{18}F; FDG).

Contrast-enhanced CT can be used to differentiate benign and malignant nodules because the intensity of enhancement is directly related to the vascularity of the nodule and to the likelihood of malignancy.[34,35] Typically, malignant nodules enhance greater than 20 Hounsfield units (HU), whereas benign nodules enhance less than 15 HU.[36] Although nodule-enhancement CT has a high negative predictive value, it is performed infrequently because of the general availability of FDG PET-CT.[37]

FDG PET allows differentiation of malignant and benign nodules that are indeterminate after conventional imaging (Fig. 2-7). A metaanalysis of 40 studies on the accuracy of FDG-PET reports a sensitivity of 97% and a specificity of 78% when used in the evaluation of 10-mm or larger nodules.[38] However, a recent prospective integrated PET-CT evaluation of 585 patients (496 malignant, 89 benign nodules) showed that although a high standardized uptake value (SUV > 4.1) was associated with a 96% likelihood of malignancy, the likelihood of malignancy was still 25% when the SUV was 0 to 2.5.[39] Furthermore, in malignant nodules that are smaller than 1 cm in diameter or have ground-glass or partially solid morphology, FDG uptake is variable and unreliable in differentiating benign from malignant nodular opacities (Fig. 2-8).[40]

Staging Lung Cancer

Staging—the assessment of the anatomic extent of non–small cell lung cancer (NSCLC)—usually determines treatment and prognosis. Clinical staging typically includes CT and, more recently, PET-CT. CT is typically used to determine the size, location, and presence of locoregional invasion of the primary tumor (T), the presence and location of nodal (N) metastasis, and intrathoracic and distant systemic metastasis (M1a, M1b).[41,42]

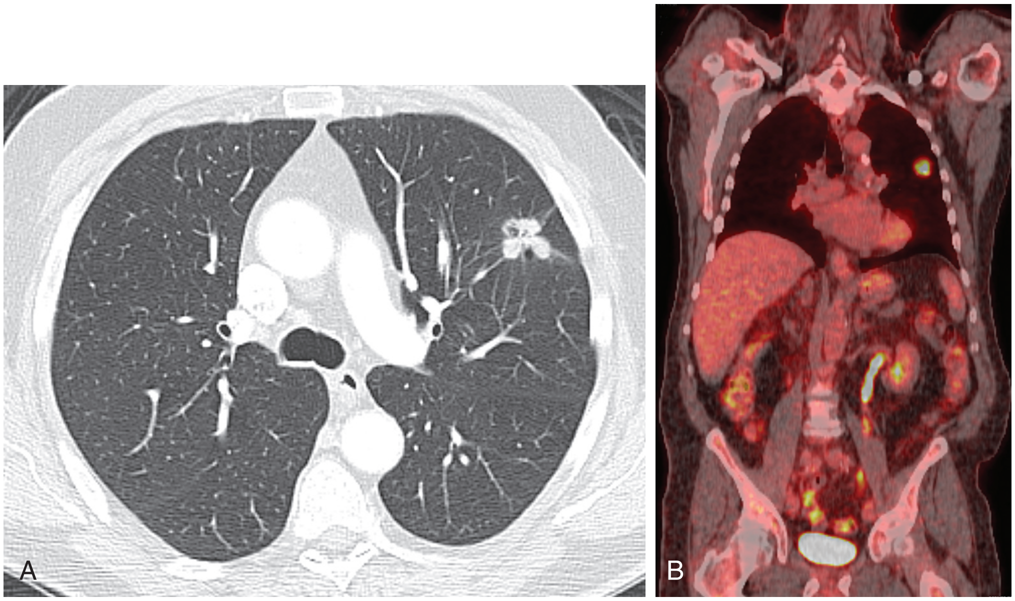

FIGURE 2-7 ■ Non-small-cell lung cancer. **A,** Axial computed tomography shows a lobular left upper lobe nodule. **B,** Fused coronal positron emission tomography–computed tomography shows small nodule in the upper lobe with increased uptake of [^{18}F] fluorodeoxyglucose, consistent with malignancy. Note the absence of nodal and distant metastases.

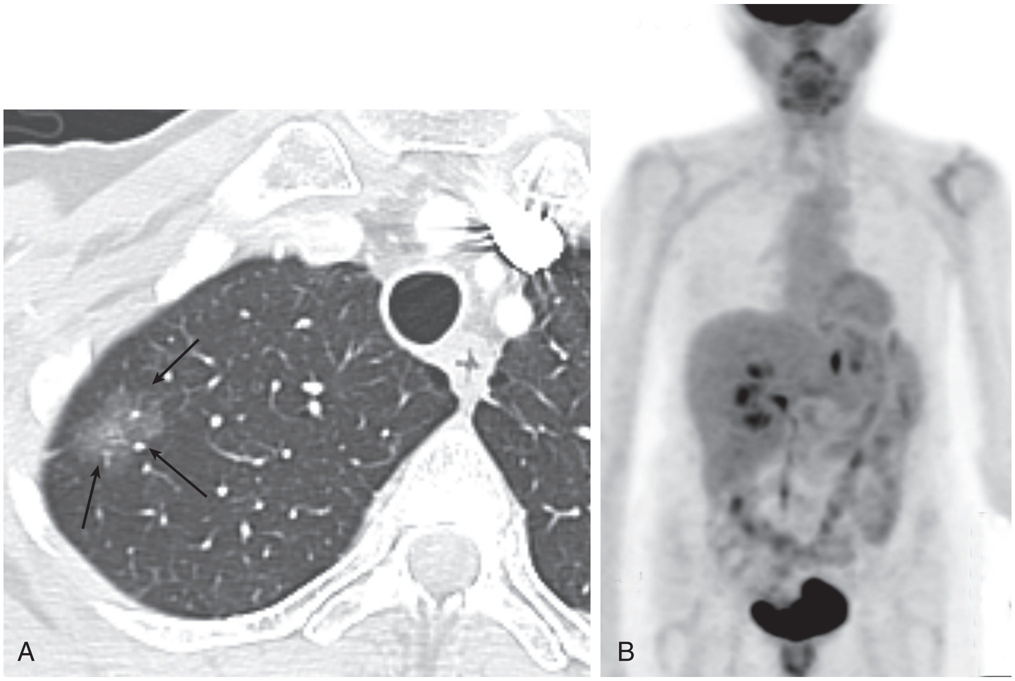

FIGURE 2-8 ■ Non-small-cell lung cancer. **A,** Axial computed tomography shows a ground glass right upper lobe lung nodule *(arrows)*. **B,** Whole body maximum intensity PET shows no uptake of [^{18}F] fluorodeoxyglucose (FDG) in the nodule. Note that FDG uptake is variable and unreliable in nodules with ground glass morphology and is not useful in differentiating benign from malignant nodules.

CT is also usually used to define chest wall or mediastinal invasion but is inaccurate in differentiating between anatomic contiguity and subtle invasion. MRI has better soft-tissue contrast resolution than CT and is useful in the evaluation of superior sulcus tumors and the brachial plexus (Fig. 2-9).[43,44]

The presence of nodal metastases and their locations are important for determining management and prognosis (Fig. 2-10).[41,42] CT is most commonly used to assess the size of nodes, and a short-axis diameter greater than 1.0 cm is the criterion typically used to diagnose nodal metastases. However, a limitation is the overlap in the size of malignant and benign lymph nodes. In this regard, a metaanalysis (20 studies, 3438 patients) evaluating CT for staging of the mediastinum yielded a pooled sensitivity of 57% and specificity of 82%.[45] PET imaging improves the accuracy of nodal staging. In a metaanalysis of 17 studies comprising 833 patients, the overall sensitivity of PET for detecting nodal metastases was 83% and the specificity was 92%, whereas the sensitivity